A Hybrid Fuzzy-Lqr Based Speed Controller for Induction Motors

Amanuel Kebebew

A Thesis Submitted to the Department of Electrical Power and Control Engineering

School Of Electrical Engineering and Computing

Presented in Partial Fulfillment of The Requirement for The Degree of Master's in Electrical Power and Control Engineering

(Control Engineering)

Office of Graduate Studies

Adama Science and Technology University

June 2023

Adama, Ethiopia

A Hybrid Fuzzy-Lqr Based Speed Controller for Induction Motors

Amanuel Kebebew

Advisor Prof. Gang Gyoo Jin

A Thesis Submitted to the Department of Electrical Power and Control Engineering Control Stream

School of Electrical Engineering and Computing

Presented in Partial Fulfillment of The Requirement for The Degree of Master's in Electrical Power and Control Engineering (Control Engineering)

Office of Graduate Studies
Adama Science and Technology University

June 2023

Adama, Ethiopia

Declaration

I hereby declare that this Master Thesis entitled "**A Hybrid Fuzzy-Lqr Based Speed Controller for Induction Motors**" is my original work. That is, it has not been submitted for the award of any academic degree, diploma or certificate in any other university. All sources of materials that are used for this thesis have been duly acknowledged through citation.

____________________	________________	______________
Name of student	**Signature**	**Date**

Recommendation of Advisors

I/we, the advisor(s) of this thesis, hereby certify that I/we have read the revised version of the thesis entitled "**A Hybrid Fuzzy-Lqr Based Speed Controller for Induction Motors**" prepared under my/our guidance by Amanuel Kebebew submitted in partial fulfillment of the requirements for the degree of Mater's of Science in Electrical Power and Control Engineering. Therefore, I/we recommend the submission of revised version of the thesis to the department following the applicable procedures.

________________	________________	________________
Major Advisor	Signature	Date
________________	________________	________________
Co-advisor	Signature	Date

Approval Page of M.Sc. Thesis

I/we, the advisors of the thesis entitled "**A Hybrid Fuzzy-Lqr Based Speed Controller for Induction Motors**" and developed by Amanuel Kebebew, hereby certify that the recommendation and suggestions made by the board of examiners are appropriately incorporated into the final version of the thesis.

________________	______________	__________
Advisor	**Signature**	**Date**
________________	______________	__________
Co-Advisor	**Signature**	**Date**

We, the undersigned, members of the Board of Examiners of the thesis by Amanuel Kebebew have read and evaluated the thesis entitled "**A Hybrid Fuzzy-Lqr Based Speed Controller for Induction Motors**" and examined the candidate during open defense. This is, therefore, to certify that the thesis is accepted for partial fulfillment of the requirement of the degree of Master of Science in Electrical Power and Control Engineering.

________________	______________	__________
Chairperson	Signature	Date
________________	______________	__________
Internal Examiner	Signature	Date
________________	______________	__________
External Examiner	Signature	Date

Final approval and acceptance of the thesis is contingent upon submission of its final copy to the Office of Postgraduate Studies (OPGS) through the Department Graduate Council (DGC) and School Graduate Committee (SGC).

________________	______________	__________
Department Head	Signature	Date
________________	______________	__________
School Dean	Signature	Date
________________	______________	__________
Office of Postgraduate Studies, Dean	Signature	Date

ACKNOWLEDGEMENTS

First and foremost, I want to praise the Almighty God, without whom the progress of this thesis would have been impossible. Next, I'd like to express my appreciation to Prof. Gang Gyoo Jin, for his professional advice, constructive remarks, ideas, and encouragement. Throughout this project, he has been a continual source of inspiration. I'd like to express my gratitude to Dr. Enadalew A. (Ph.D.) for his invaluable assistance, guidance, and support. I'd also want to express my gratitude to the members of the Electrical Power and control Engineering department for their continuous encouragement during the thesis progress. Finally, I'd want to express my gratitude to my mother, Fikre Gemechu. as well as my family and friends, who have always encouraged me to finish my work.

Table of Contents

Contents

Declaration i
Recommendation of Advisors ii
Approval Page of M.Sc. Thesis iii
ACKNOWLEDGEMENTS iv
Table of Contents v
List of Figures vii
List of Tables ix
List of Acronyms and Abbreviations x
ABSTRACT xi
INTRODUCTION 1
1.1 Background of Study 1
1.2 Statement of the Problem 2
1.3 Objectives 2
1.3.1 General objective: 2
1.3.2 Specific objectives: 2
1.4 Significance of the Study 3
1.5 Scope of Study 3
CHAPTER TWO 4
LITERATURE REVIEW 4
2.1 Background 4
CHAPTER THREE 9
MATERIALS AND METHODS 9
3.1 Materials 9
3.1.2 Software tools 9
3.2 Methods 10
3.2.1 Construction of Induction Motor 10
3.2.2 Operation of Induction motor 11
3.2.3 Mathematical Model 12
3.2.4 Reference Current Generator 16
3.2.5 Hysteresis Current Control 17

3.2.6 Mathematical Model of Voltage Source Inverter (VSI) 18
3.2.7 Field Oriented Control Methods 21
3.2.8 Controller Design 25
CHAPTER FOUR 41
RESULTS AND DISCUSSIONS 41
4.1 Introduction 41
4.2 Simulink Model of the Drive System 41
4.2.1 Voltage equation model 43
4.2.2 Commutation Logic Model 44
4.2.3 Field Oriented Control Sub-Blocks 45
4.2.4 LQR controller Model 48
4.2.5 FLC controller model 49
4.3. Results and discussions 49
4.3.1 Result of LQR based Induction motor controller 50
4.3.2 Result of Fuzzy-logic based Induction motor speed control 54
4.3.3. Result of Fuzzy-LQR based Induction motor speed control 58
CONCLUSIONS AND RECOMMENDATIONS 63
Conclusion 63
Recommendation 64
References 65
APPENDIX lxviii

List of Figures

Figure 3.1 Block diagram of an induction motor drive system 9
Figure 3.2 Construction of Three phase Induction motor 11
Figure 3.3 A dq0 equivalent circuit of an Induction Motor 13
Figure 3.4 PWM current controller image... 17
Figure 3.5 Voltage drop on one inverter leg... 19
Figure 3.6 Model of Real Voltage Source Inverter (VSI) 20
Figure 3.7 Ideal two-level three-phase voltage source inverter (VSI) 21
Figure 3.8 Magnitude and position of the rotor flux vector using Hall sensors and a rotor flux calculator 22
Figure 3.9 Indirect field oriented control scheme... 24
Figure 3.10 Block diagram of LQR controlled IM drive 26
Figure 3.11 [a] Triangular MF, [b] Trapezoidal and [c] Bell membership function........... 33
Figure 3.12 Structure of fuzzy membership function.. 33
Figure 3.13 Fuzzy logic speed control of Induction motor 35
Figure 3.14 Membership function plot for input variable "Error"..................................... 36
Figure 3.15 Membership function plot for input variable "Error Change"......................... 37
Figure 3.16 Membership function plot for output variable "Output" 37
Figure 3.17 The system's fuzzy inference system 38
Figure 3.18 Surface view of the generated rules 38
Figure 3.19 Generated rules using the two inputs and an output 39
Figure 3.20 Rule view of the generated rules.. 40
Figure 4.1 The general structure of fuzzy-LQR controlled Induction motor drive............ 43
Figure 4.2 Voltage equation 43
Figure 4.3 Inverter function model.. 44
Figure 4.4 Field oriented control SIMULINK model.. 45
Figure 4.5 Field oriented control SIMULINK model.. 45
Figure 4.6 Rotor flux magnitude calculation... 46
Figure 4.7 Theta calculation 46
Figure 4.8 SIMULINK model to calculate the direct current reference component $Ide*$. 47
Figure 4.9 SIMULINK model to calculate quadrature current reference component $Iqe*$ 47
Figure 4.10 Convert current components in rotating frame to three-phase currents in stationary frame 47

Figure 4.11 SIMULINK model of current regulator 48
Figure 4.12 Shows how the optimal gain matrix Kopt modeled on Simulink 48
Figure 4.13 FLC for the Induction motor drive system's outer speed loop 49
Figure 4.14 Simulink diagram for LQR based Induction motor control 50
Figure 4.15 Reference speed and actual speed for LQR controlled Induction motor 51
Figure 4.16 Electromagnetic Torque for LQR controlled Induction motor 51
Figure 4.17 Speed Tracking Error 52
Figure 4.18 Phase stator currents... 52
Figure 4.19 Per-phase stator currents 53
Figure 4.20 Simulink diagram for FLC based Induction motor control............................. 54
Figure 4.21 Reference speed and actual speed for Fuzzy controlled Induction motor 55
Figure 4.22 Electro Magnetic Torque for Fuzzy controlled Induction motor 55
Figure 4.23 Speed Tracking Error 56
Figure 4.24 Stator phase currents for Fuzzy controlled Induction motor............................ 56
Figure 4.25 Per-phase Stator currents for Fuzzy controlled Induction motor 57
Figure 4.26 Simulink diagram for Fuzzy-LQR based Induction motor control.................. 58
Figure 4.27 Reference speed and actual speed for Fuzzy-LQR controlled Induction motor 59
Figure 4.28 Speed Tracking error... 59
Figure 4.29 Three phase stator current 60
Figure 4.30 Per-Phase Stator Currents Ia,Ib and Ic 60
Figure 4.31 Electromagnetic Torque of Fuzzy-Lqr controller 61

List of Tables

Table 3.1 Reference currents corresponding to rotor position signals 16
Table 3.2 Fuzzy membership functions and their symbols 36
Table 3.3 Rule base table for the drive system.. 37
Table 3.4 Lists the Induction motor parameters 42
Table 3.5 List of performance attained by each controller.. 62

List of Acronyms and Abbreviations

AC: Alternating Current

BLDC: Brushless Direct Current

DC: Direct Current

DC-DC: Direct Current to Direct Current

DTC: Direct Torque Control

FLC: Fuzzy Logic Controller

IM:Induction Motor

LQR: Linear Quadratic Regulator

PI: Proportional Integral

PID: Proportional Integral Derivative

RMF: Rotating Magnetic Field

SMC: sliding mode control

SVPWM: Space Vector Pulse Width Modulation

ABSTRACT

Induction motors are now widely utilized in a variety of industrial and household applications due to their benefits, which include simple construction, rugged, high reliability and high efficiency. Despite the benefits, an Induction motor has uncertain and nonlinear characteristics which degrade the performance of controllers. As a result, many controllers fail to smoothly track the speed trajectory. Therefore, appropriate speed controllers are required to attain the required level of performance. In this thesis, the Fuzzy- linear quadratic regulator Control technique is used for the speed control of the Induction motor drive system. The proposed control technique is designed, and its performance evaluated against the linear quadratic regulator and the fuzzy logic controller individually. A set of simulation works have been done using MATLAB/SIMULINK. The simulation results show that linear quadratic regulator alone produces a smooth speed response with better rise time and overshoot but it is aggressive and produces chattering about the desired value. The fuzzy logic, on the other hand, with the better settling time and overshoot but high rise time value when it compared to others it is also unable to completely eliminate disturbance. The proposed Fuzzy-Linear quadratic regulator technique takes the benefits of both linear quadratic regulator and Fuzzy controllers to improve the motor drive system's dynamic behavior and it is more resistant to load perturbations (disturbance). The Fuzzy-Linear quadratic regulator controller reduced the overshoot eliminated the chattering effect and resulted in smooth speed tracking with optimal control force utilization, which is the main objective of this thesis.

Keywords*: - Induction motor, Fuzzy Logic controller, Linear quadratic regulator, Fuzzy-Linear quadratic regulator controller, MATLAB/ SIMULINK*

CHAPTER ONE
INTRODUCTION

1.1 Background of Study

Induction machines are also called asynchronous machines are the most used electrical machines in the industry. In fact, induction motors are so common in industry that in many plants no other type of electric machine can be found. Since Induction motors are available as single-phase or three-phase. Therefore, it is important to study induction motor for better understanding since its essential role in the industry (Zaparoli, 2020). Single phase induction motors generally have a construction similar to that of a three phase motor: an ac windings is placed on the stator, short-circuited conductors are placed in a cylindrical rotor. The significant difference is, of-course, that there is only a single-phase supply to the stator (Lipo, 2017).To improve the performance of Induction motor drives, many machine design and control schemes have been developed. In the development of the control schemes, controllers' adaptation in the system has become compulsory in various domains, as the advantage it provides is of in large scale. The controllers like PI, PID, LQR, fuzzy logic and SMC are mainly discussed in many papers. Among the above-mentioned control algorithms, PID and LQR controllers can be mainly used for linear systems whereas Fuzzy and SMC controller can also be applied in nonlinear systems. LQR is an optimal controller that minimizes the quadratic cost functions which integrate both states and inputs of the system via penalty matrices. It offers an optimal response between speed of response and amount of control input through cost function minimization. The inherent stability and robustness characteristics of LQR guarantee the stability of many systems (Kumar, 2020, June). On the other hand, faster dynamic responses are obtained when nonlinear controllers are placed in power electronic controlled systems. There are many nonlinear controllers like current mode controller, one-cycle control, fuzzy logic controller, sliding mode controller which are employed for DC-DC converters. Amongst all those mentioned, fuzzy logic controller and SMC are advantageous as they are simple and model free techniques. Plant uncertainties and external disturbances are two major problems for systems, to make system free from those two issues, fuzzy logic controller (FLC) is projected because of its inherent advantages such as requirement of only approximate data, simple cost-effective sensors and robustness. Moreover, Fuzzy algorithms are quite understandable and healthy. Thus, the system now becomes independent of effects due to modeling uncertainties, parameter fluctuations and disturbances.

1.2 Statement of the Problem

In comparison to induction motors and ordinary brushed DC motors, Induction motors have several benefits. Which includes low maintenance, high life expectancy, simple construction, high speed application, can be used in large industries, and noiseless operations are just a few of the benefits. These motors are extensively utilized in several applications such as aerospace, automotive, medical, instrumentation, robotics, actuation, industrial automation equipment, machine tools, and so on, due to their advantageous electrical and mechanical features they have been used for enhancing our way of doing things. Despite these benefits, induction motor systems have uncertain and nonlinear characteristics in their speed that decrease controller performance especially under disturbed condition which is when we add more load to Induction motor. As a result, many controllers fail to track the motor's speed trajectory properly smoothly and effectively as required. So, in this paper I used a hybrid Fuzzy-LQR control technique to solve these difficulties which are maximum torque and efficiency problem then improve the uncertainty and non-linearity characteristics of speed.

1.3 Objectives

1.3.1 General objective:

The general objective of this study is to develop the speed controller for an induction motor using the hybrid Fuzzy-LQR technique.

1.3.2 Specific objectives:

1. To model the induction motor.
2. To design the LQR based controller for the induction motor.
3. To design fuzzy logic controller for the Induction motor.
4. To design hybrid Fuzzy-LQR based controller for the induction motor.
5. To evaluate their speed control performances

1.4 Significance of the Study

As we know induction motors are commonly employed in several applications such as instrumentation, actuation, robotics, automotive, aerospace, medical, machine tools, and industrial automation and so on. Developing the proposed Fuzzy-LQR control technique will best enhance the motor performance by handling a speed control problems of the motor like model uncertainty and optimization problem, accomplishing better speed control and minimizing error. This results in the overall improvement of the system in which the motor installed.

1.5 Scope of Study

This study obtains at the mathematical modeling of an induction motor using differential equations. It also comprises the design of LQR, which necessitates a cost function optimization that balances the speed of the system reaction with the cost of the amount of control force (input) provided through an Engineering tradeoff. There will be a Fuzzy logic controller that is intelligent and basically the IF-THEN rules can be best utilized in designing a controller. Finally, this research included simulation software such as MATLAB/SIMULINK. The experimental validation of the proposed controller architecture will be restricted to MATLAB simulation only owing to the unavailability of drive system hardware components to conduct practical testing.

CHAPTER TWO

LITERATURE REVIEW

2.1 Background

The work of this study is necessary based on what has been already done by other researchers on topics related to the work. So as to look into the works of these scholars and get necessary and important information related to the topic, different literature will be referred from different available sources such as books, papers, journals, internets, and others.

In this section, a review of related literature describing the modeling of Induction motor, fuzzy logic and LQR based speed control systems were presented. More specifically, the related previous studies and researches on modeling and speed control strategies applied to induction motor speed are presented.

Vaibhavi R. Metha and Shushil S. Karvekar (Metha, 2018, October) studied Speed Control of Induction Motor using a Fuzzy Logic Controller and Direct Torque Controller. This paper proposes a Direct Torque Control (DTC) for three-phase induction motor using Fuzzy Logic Controller (FLC) an alternative for the traditional PI controller. The DTC has some special features like no feedback current control and vector transformation. This method gives an excellent dynamic response with a simple structure. Since the DTC experiences a high torque and flux ripples due to the use of the PI controller but using FLC gives an advantage to reduce flux and torque ripples. An FLC assures definite speed tracking and gradually improves the robustness against ambiguity and disturbances. The effectiveness of the presented method is analyzed with the help of simulation results.

Sharad Chandra Rajpoot, Neeraj Kumar Soni, Sudeep Shrivastava and Prashant Singh Rajpoot (Rajpoot, 2018) studied Speed control of three phase motor using fuzzy logic controller. In this paper Fuzzy logic controller based speed control of a three phase induction motor. The system is modeled in a MATLAB/SIMULINK and the result is being compared with the conventional PI controller. Constant v/f control scheme is being implemented in the scheme. The controller is designed such that it can reduce the error between rotor speed and reference speed as fast as possible. The performance of the controller with the change in reference speed is simulated and the dynamic performance of the motor is observed. Result show that the dynamic performance of the induction motor is improved. Along with that result shows that the system is not much affected to the disturbance occurring in the system. The induction motor attains adaptability to the system disturbances which proves to be very useful for the robust performance of the motor.

Manoj Swargiary, Jayati Dey and Tapas Kumar Saha (Swargiary, 2017, September) studied optimal speed control of induction motor based on Linear Quadratic Regulator theory. In this paper, the optimal speed control, based on Linear Quadratic Regulator (LQR) theory, through stator field orientation (SFO) of an inverter fed induction motor is addressed. The voltage source inverter, behaving as an actuator, is operated using space vector pulse width modulation (SVPWM) technique. The state feedback system is augmented with integral output error to enhance reference tracking and disturbance rejection criteria. In addition, a feed forward gain is introduced to ensure unity dc gain in case of reference tracking. The LQR synthesis is carried out for the whole system considering the integral output error as an additional state. It is interesting to note that the structure of the control law used here resembles the classical proportional integral control law.

Beddiaf.Yassine, Zidani Fatiha and Larbi Chrifi-Alaoui (Yassine, 2019, March) studied Robust speed sensorless indirect field-oriented control of induction motor drive using LQR controller. In this paper, to achieve accurate performance of speed control of IM, a newly designed optimal control method is presented. The new proposed controller is designed by combining PI controller and LQR. This is a new technique fully matches the merits of the easy design of the LQR and the strong robustness of the PI. Simulation results and experimental results show that the proposed approach gives good results. So, the similarity between this project and my proposal is that both are used for speed control of IM, but the main difference is in this project Robust speed sensor less indirect field-oriented control of induction motor drive using LQR for speed control but in my proposal the hybrid method of LQR and FLC will be applicable.

S Usha and C Subramani (Usha, 2018) studied the speed control of the parallel connected system is performed by PID controller and fuzzy logic controller. In this paper the speed response of the induction motor for the rating of IHP, 1440 rpm, and 50Hz with this controller are compared in time domain specifications. The stability analysis of the system also performed under low speed using Matlab platform. The hardware model is developed for speed control using fuzzy logic controller which exhibited superior performances over the other controller.

P. Upendra Kumar,J. Harish and M. Ram Babu (Upendra, 2016) studied Then PID control technique is applied to the considered induction motor along with LQR control law is also designed for the obtained linearized system. The non-linear plant dynamics are linearized by using dynamic feedback linearization techniques. By providing all these aspects, the speed control of induction motor is achieved in a wide range. To observe speed control, sinusoidal Ramp and Linear signals were taken as reference. Simulations are carried out and the performances of the designed controllers are compared. The design of these controllers is implemented in MATLAB/SIMULINK software.

S. Senthilkumar and S. Vijayan (Senthikumar, 2013) presented a PID controller for three phase induction motor using V/F method. The used control scheme is based on constant volts per hertz ratio and using the high Performance PID controller. Design of induction motor mathematical modeling and PID controller for Space Vector Pulse Width Modulation inverter are proposed for induction motor V/f speed control. The simulation is carried out by MATLAB/Simulink.

Yakala Satyanarayana and Dr.A.Srujana (Satyanarayana, 2012) this paper presents design and implements a voltage source inverter type space vector pulse width modulation (SVPWM) for control a speed of induction motor. This paper also introduces a fuzzy logic controller to the SVPWM in order to keep the speed of the motor to be constant when the load varies. FLC is used to control the pulse width of the PWM converter used to control the speed of the motor. The simulation is carried out by MATLAB/Simulink.

Anmol Aggarwal, J. N. Rai and Maulik Kandpal (Aggarwal, 2015) the main objective of this paper is to develop a fuzzy logic based controller to control the speed of the induction motor, employing the scalar control model. The voltage and frequency input to the induction motor are to be controlled in order to obtain the desired speed response. The designed Fuzzy Logic Controllers performance is also weighed against with that of a PI controller. For V/f speed control of the induction motor, a reference speed has been set and the control architecture includes a rule base of 49 rules. These rules portray a nonchalant relationship between two inputs i.e. speed error (e), change in speed error (Δe) and an output i.e. change of control (ω_{sl}). The simulation is carried out by MATLAB/Simulink.

Betsega Yosef (Betsega, 2021) mentioned that Feedback linearization technique is used to linearize both the translational and rotational dynamics. Here during linearization an auxiliary control inputs arises and those linear control inputs are found through linear control technique called linear quadratic regulator. Constant trajectory tracking and rectangular trajectory tracking is also obtained by controlling the attitude and the position simultaneously. The simulation is carried out by MATLAB/Simulink.

Basem M. Badr, Ali M. Eltamaly and A. I. Alolah (Badr, 2010) in this paper Induction motor is modeled in synchronous reference frame in terms of *dq* form. The speed control of induction motor is the main issue achieves maximum torque and efficiency. Two speed control techniques, Scalar Control and Indirect Field Oriented Control are used to compare the performance of the control system with fuzzy logic controller. Indirect field-oriented control technique with fuzzy logic controller provides better speed control of induction motor especially with high dynamic disturbances. The model is carried out using Matlab/Simulink computer package.

Ahmed Fattah in thesis hybrid PID-Fuzzy control system for the speed control of a three-phase squirrel cage induction motor. The design of fuzzy system consists of 9 fuzzy variables and 49 IF-THEN rules that define the behavior of the system. The FLC observes the loop error signal and correspondingly control the PID input error signal so that the actual speed signal matches the reference speed signal with reduced rise time, settling time, and peak over shoot. Implementation and simulation results using MATLAB/SIMULINK

Research Gap

Compared to Vaibhavi R. Metha and Shushil S. Karvekar (Metha, 2018, October) paper they worked on speed control of induction motor DTC with the use of fuzzy with no feedback control which is simple in construction and also useful for operating different disturbances but these system have some limitation which are the hybrid controller may not provide significantly improved performance in removing non linearity and uncertainty of speed over either fuzzy logic control or DTC alone. In some cases, it may be more effective to use one method over the other.

Compared to Sharad Chandra Rajpoot, Neeraj Kumar Soni, Sudeep Shrivastava and Prashant Singh Rajpoot paper they worked on speed control of induction motor by using Fuzzy Logic controller the major advantage of using these method is the ability to operate under disturbed condition but their also limitation use of these system The problem with this FLC controller is that The performance of a fuzzy logic controller depends heavily on the choice of membership functions and rules. If these are not properly designed, the controller may not provide the desired performance which is eliminating disturbance and remove nonlinearity and uncertainty of speed.

CHAPTER THREE

MATERIALS AND METHODS

3.1 Materials

In this chapter, mathematical modeling of the components of the induction motor drive is discussed. The induction motor drive system generally consists of five main components: the AC power supply, the induction motor, the AC-DC and DC-AC converter, the control unit, and the Sensor. All these components are presented together with their mathematical models in detail in this chapter.

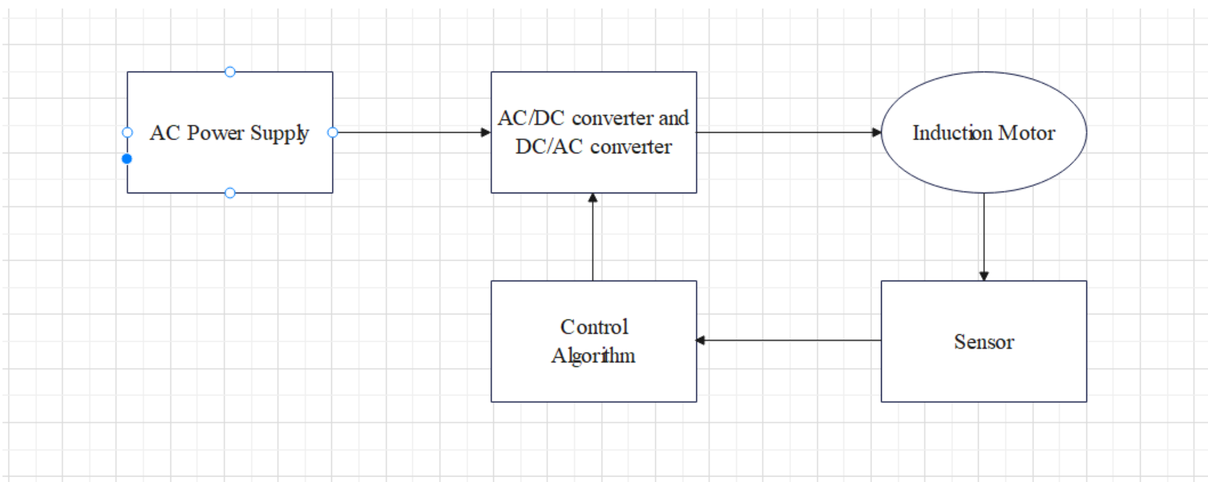

Figure 3.1 Block diagram of an induction motor drive system

3.1.2 Software tools

Simulation will be carried by using MATLAB/SIMULINK to model the induction motor ,to design LQR(Linear Quadratic regulator) speed controller, to design FLC(Fuzzy Logic Controller) speed controller , to design hybrid FUZZY-LQR speed controller and finally all the simulation result will be viewed then from this simulation result we will try to evaluate and compare the results of hybrid Fuzzy-LQR speed controller with FLC and LQR controller based on this we will try to determine which method is more enhanced for speed control of Induction motor. The other software used is EdrawMax for creating block diagrams for drive system of induction motor also for making block diagram for LQR controlled IM drive system, FLC IM drive system and finally to make block diagram for Fuzzy-LQR drive system for speed control of induction motor. Finally Microsoft word is used for writing all data, images, and block diagrams in best understandable way.

3.2 Methods

3.2.1 Construction of Induction Motor

The stator and rotor are the main parts of the induction machine. The stator has three main parts: Outer frame, Stator core and Stator winding. The outer frame or motor housing is the outer body of the motor. Its function is to support the stator core and to protect the inner parts of the machine against mechanical impacts. The stator core is made of thin, soft-iron laminations varies from 0.3 to 0.5 mm in thickness stacked and screwed together to minimize hysteresis and eddy current losses. Furthermore, each lamination is insulated from the other with a thin varnish layer on both sides for better insulating. Slots are punched on the inner periphery of the stampings. Stator winding are three phase winding carried on the stator core where the six terminals of the winding are connected in the terminal box of the machine. Therefore, the three-phase winding could be connected in star or delta. Rotor is the rotating part of the motor. It has cooling fins. At the back, there is another bearing and a cooling fan affixed to the rotor. The fan is enclosed by a fan cover. There are two types of rotors, Squirrel cage rotor and Phase wound rotor. Most of the induction motors employed in the industry have squirrel cage rotor Due to its simple and robust construction. It consists of a laminated cylindrical core having semi-closed circular slots at the outer periphery. Copper or aluminum bar conductors are placed in these slots and short circuited at each end by copper or aluminum rings. Thus, the rotor winding is permanently short-circuited and no external resistance can be added in the rotor circuit. The slots are skewed compared to the shaft to obtain smooth and sufficient torque and reduces the magnetic locking of the stator and rotor increases the rotor resistance since the length of the rotor bar conductors is increased.

On the other hand, Phase wound rotor consists of stamping as in stator core. A number of semi-closed slots are punched at its outer periphery. A 3-phase insulated winding is placed in these slots. The rotor is wound for the same number of poles as that of stator. The rotor winding is connected in star and its remaining three terminals are connected to the slip rings. In this case, any external resistance can be added in the rotor circuit. The rotor is also skewed as in squirrel cage rotor. Finally, a shaft is fixed to the rotor to transfer mechanical power

(Lipo, 2017), (Kumar, 2020, June).

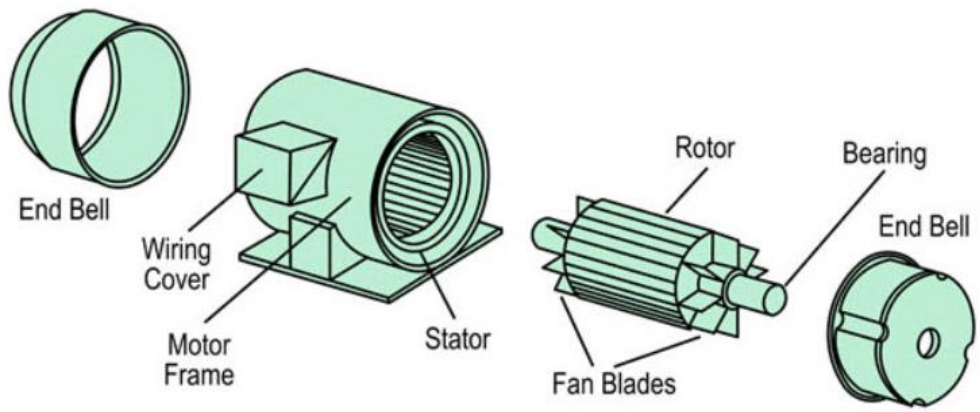

Figure 3.2 Construction of Three phase Induction motor (Neupane, 2023)

3.2.2 Operation of Induction motor

In an induction motor only the stator winding is fed with an AC supply. Alternating flux is produced around the stator winding due to AC supply. This alternating flux revolves with synchronous speed. The revolving flux is called as "Rotating Magnetic Field" (RMF).The relative speed between stator RMF and rotor conductors causes an induced emf in the rotor conductors, according to the Faraday's law of electromagnetic induction. The rotor conductors are short circuited, and hence rotor current is produced due to induced emf. That is why such motors are called as induction motors. (This action is same as that occurs in transformers, hence induction motors can be called as rotating transformers.) Now, induced current in rotor will also produce alternating flux around it. This rotor flux lags behind the stator flux. The direction of induced rotor current, according to Lenz's law, is such that it will tend to oppose the cause of its production. As the cause of production of rotor current is the relative velocity between rotating stator flux and the rotor, the rotor will try to catch up with the stator RMF. Thus, the rotor rotates in the same direction as that of stator flux to minimize the relative velocity. However, the rotor never succeeds in catching up the synchronous speed (Dias, 2022).

3.2.3 Mathematical Model

The mathematical model of the drive system is necessary for analyzing and studying the entire system's behavior. When modeling the Induction motor drive, we need take into account its structure and operating modes. The modeling’s of the components that make up the drive system were covered in depth in this topic.

3.2.3.1 Induction Motor model

An Induction motor's model equations are made up of a voltage equation, a torque equation, and a motion equation. Generally, three phase stator windings and a rotor make up the Induction motors. When modeling and controlling an Induction motor, the following assumptions are taken into consideration.

i. Uniform air gap.
ii. Squirrel cage type construction.
iii. Balanced stator and rotor windings, with sinusoidally distributed winding.
iv. Saturation and parameter change are neglected.

The steady state model and equivalent circuit of the Induction Motor is useful for studying the performance of the machine in steady state. This implies that all electrical transients are neglected during load changes or stator frequency variations. Such variations arise in application involving variable-speed drives. The variable-speed drives are converter fed from finite sources, unlike the utility sources, due to limitations of the switch ratings and filter sizes. This results in their incapability to supply large transient power. Hence, we need to evaluate the dynamics of converter-fed variable-speed drives to assess the adequacy of the converter switches and the converters for a given number of motor and their interaction to determine the excursions of currents & torque in the converter and motor (Leedy, 2022, April).

Equivalent Circuit of an Induction Motor

The voltage and torque equations that describe the dynamic behavior of an induction motor are time-varying. It is successfully used to solve such differential equations and it may involve some complexity. A change of variables can be used to reduce the complexity of these equations by eliminating all time-varying inductances, due to electric circuits in relative motion, from the voltage equations of the machine (Rajput, 2020).

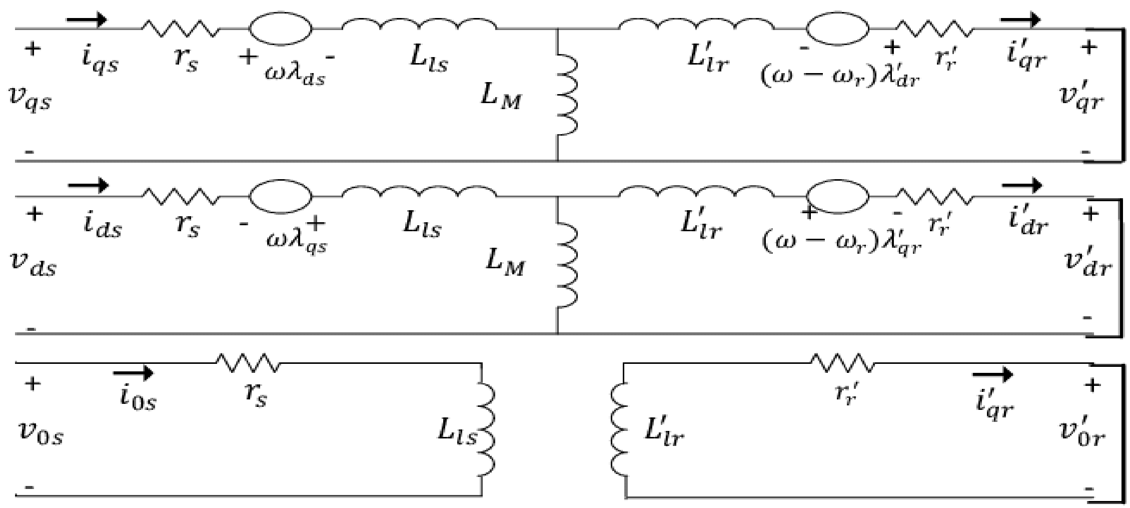

Figure 3.3 A dq0 equivalent circuit of an Induction Motor (Aktaibi, 2011)

The above figure shows a dq0 equivalent circuit of an Induction motor. The circuit comprise of various time varying inductances which are to be simulated to analyze the dynamic performance of the 3-phase Induction motor.

Generalized Concept in an Arbitrary Reference Frame

Reference frame are very much like observer platforms, in that each of the platforms gives a unique view of the system at hand as well as a dramatic simplification of the system equation. For example, for the purpose of control, it is desirable to have the system variables as dc quantities, although the actual variables are sinusoidal. This could be accomplished by having a reference frame revolving at the same angular speed as that of the sinusoidal variable. As the reference frames are moving at an angular speed equal to the angular speed equal to angular frequency of sinusoidal supply, so that differential speed between them is reduced to zero, resulting in the sinusoid signal behaving as DC signal from the reference frames. So, by moving that lane, it becomes easier to develop a small-signal equation out of a non-linear equation, as the operating point is described only by DC values; this then leads to linearized system around operating point. Such advantages are many from using reference frames. Instead of deriving the transformation for each and every particular reference frame; it is advantageous to derive general transformation for an arbitrary rotating reference frame. Then any particular reference frame model can be derived by substituting the appropriate frame speed and position in the generalized reference model.

Three-phase to Two phase Transformation

The dynamic model of induction motor can be derived if the equivalence between three-phase and two-phase machine is studied. The equivalence is based on the quantity of MMF produced in two-phase and three-phase windings along with equal current magnitudes. Assuming that each of the three-phase winding has Ns turns per phase and equal currents magnitudes, the two-phase winding will have $3Ns/2$ turns per phase for MMF equality. The d and q axes MMF are found by resolving MMF of the three-phase along d and q axes. The common term, the number of turns is cancelled on both sides of equations leaving behind the current equalities. The three-phase stator voltages of an induction machine under balanced conditions can be expressed as

$$\begin{aligned} V_a &= \sqrt{2}V_{rms}\sin(\omega t) \\ V_b &= \sqrt{2}V_{rms}\sin(\omega t - 2\pi/3) \\ V_c &= \sqrt{2}V_{rms}\sin(\omega t + 2\pi/3) \end{aligned} \tag{3.1}$$

Here V_a, V_b *and* V_c are the three-line voltages. The relationship between $\alpha\beta$ and abc is as follows.

$$\begin{bmatrix} V_\alpha \\ V_\beta \end{bmatrix} = \frac{2}{3}\begin{bmatrix} 1 & \frac{1}{2} & -\frac{1}{2} \\ 0 & \frac{\sqrt{3}}{2} & -\frac{\sqrt{3}}{2} \end{bmatrix}\begin{bmatrix} V_a \\ V_b \\ V_c \end{bmatrix} \tag{3.2}$$

Then, the direct and quadrature axes voltages are:

$$\begin{bmatrix} V_d \\ V_q \end{bmatrix} = \begin{bmatrix} \cos\theta & \sin\theta \\ -\sin\theta & \cos\theta \end{bmatrix}\begin{bmatrix} V_\alpha \\ V_\beta \end{bmatrix} \tag{3.3}$$

The instantaneous values of the stator and rotor currents in three-phase system are ultimately calculated using the following transformation.

$$\begin{bmatrix} i_\alpha \\ i_\beta \end{bmatrix} = \begin{bmatrix} \cos\theta & -\sin\theta \\ \sin\theta & \cos\theta \end{bmatrix}\begin{bmatrix} i_d \\ i_q \end{bmatrix} \tag{3.4}$$

$$\begin{bmatrix} i_a \\ i_b \\ i_c \end{bmatrix} = \frac{2}{3}\begin{bmatrix} 1 & 0 \\ -\frac{1}{2} & -\frac{\sqrt{3}}{2} \\ -\frac{1}{2} & -\frac{\sqrt{3}}{2} \end{bmatrix}\begin{bmatrix} i_\alpha \\ i_\beta \end{bmatrix} \tag{3.5}$$

Equations of Flux Linkages & Simulink Model

The dynamic model of induction motor in arbitrary reference frame can be represented by using flux linkages as variables. This involves the reduction of a number of variables in dynamic equations, which greatly facilitates their solution by using analogue and hybrid computers. Even when the voltages and currents are discontinuous, the flux linkages are continuous. This gives the advantage of differentiating these variables with numerical stability. In addition, the flux linkages representation is used in motor drives to highlight the process of the decoupling of the flux and torque channels in the induction and synchronous machine. The various flux linkage equations are expressed as,

$$\begin{aligned}
\frac{d\lambda_{qs}}{dt} &= \omega_b\left[V_{qs} - \left(\frac{\omega_e}{\omega_b}\right)\lambda_{ds} - \left(\frac{R_s}{X_{ls}}\right)(\lambda_{mq} - \lambda_{qs})\right] \\
\frac{d\lambda_{ds}}{dt} &= \omega_b\left[V_{ds} - \left(\frac{\omega_e}{\omega_b}\right)\lambda_{ds} - \left(\frac{R_s}{X_{ls}}\right)(\lambda_{md} - \lambda_{ds})\right] \\
\frac{d\lambda_{qr}}{dt} &= \omega_b\left[V_{qr} - \left(\frac{\omega_e - \omega_r}{\omega_b}\right)\lambda_{dr} - \left(\frac{R_r}{X_{lr}}\right)(\lambda_{mq} - \lambda_{qr})\right] \\
\frac{d\lambda_{dr}}{dt} &= \omega_b\left[V_{dr} - \left(\frac{\omega_e - \omega_r}{\omega_b}\right)\lambda_{qr} - \left(\frac{R_r}{X_{lr}}\right)(\lambda_{md} - \lambda_{dr})\right]
\end{aligned} \tag{3.6}$$

Where

$$\lambda_{mq} = X_{ml}\left[\frac{\lambda_{qs}}{X_{ls}} + \frac{\lambda_{qr}}{X_{lr}}\right] \tag{3.7}$$

$$\lambda_{md} = X_{ml}\left[\frac{\lambda_{ds}}{X_{ls}} + \frac{\lambda_{dr}}{X_{lr}}\right] \tag{3.8}$$

Then substituting the values of the flux linkages to find the currents,

$$i_{qs} = \frac{1}{X_{ls}}(\lambda_{qs} - \lambda_{mq}) \tag{3.9}$$

$$i_{qr} = \frac{1}{X_{lr}}(\lambda_{qr} - \lambda_{mq})$$
$$i_{ds} = \frac{1}{X_{ls}}(\lambda_{ds} - \lambda_{md}) \tag{3.10}$$
$$i_{dr} = \frac{1}{X_{lr}}(\lambda_{dr} - \lambda_{md})$$

Based on the above equations, the Electromagnetic torque and rotor speed can be determined as follows,

$$T_e = \left(\frac{3}{2}\right)\left(\frac{P}{2}\right)\left(\frac{1}{\omega_b}\right)\left(\lambda_{ds}i_{qs} - \lambda_{qs}i_{ds}\right)$$
$$\omega_b = \int\left(\frac{P}{2J}\right)(\mathrm{T}_e - \mathrm{T}_l) \tag{3.11}$$

With P = no of poles of Machine. Te= Electromagnetic torque developed (Goolak,2020).

3.2.4 Reference Current Generator

The magnitude of the three-phase current i_{ref} is determined by using reference torque T_{ref}

$$i_{ref} = \frac{T_{ref}}{K_t} \tag{3.12}$$

Where, K_t is the torque constant. The reference current generator block produces three-phase reference currents 0(i_a , i_b , i_c) based on the rotor position by using the value of Reference current magnitude as i_{ref}. The reference current for each phase i_a^*, i_b^*, i_c^* are functions of the rotor position (Babu, 2019). Rotor position signal and Reference currents are shown in Table 3.1.

Table 3.1 Reference currents corresponding to rotor position signals

Rotor Position(θ_r)	i_a^*	i_b^*	i_c^*
0-60	i_{ref}	$-i_{ref}$	0
60-120	i_{ref}	0	$-i_{ref}$
120-180	0	i_{ref}	$-i_{ref}$
180-240	$-i_{ref}$	i_{ref}	0

240-300	$-i_{ref}$	*0*	i_{ref}
300-360	*0*	$-i_{ref}$	i_{ref}

3.2.5 Hysteresis Current Control

In order to generate the switching signals for the inverter, a hysteresis current controller is utilized. Hysteresis PWM is a type of instantaneous feedback current control in which the real current follows the reference current within the hysteresis band. Figure 3.4 shows the operating principle of hysteresis band pulse width modulation for half bridge inverter. The control circuit generates the pulsating sinusoidal reference current. The reference current is then compared with actual phase current wave. When the actual current exceeds the reference current, the upper switch is off and lower switch is on (Lam, 2020).

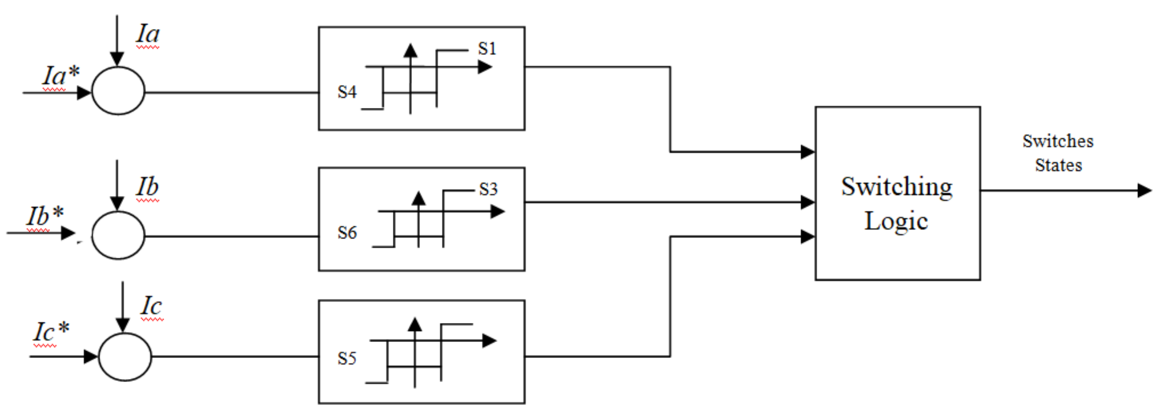

Figure 3.4 PWM current controller image (Kalyanraj, 2014)

On the other hand, when the reference current exceeds the actual current, the upper switch is turned on and the lower switch is turned off, similar to how the other phases are controlled. These switches are applied to the PWM inverter gates as shown in figure 3.6

The switching logic is formulated as:

If ia < ia∗ switch 1 is turned ON and switch 4 is turned OFF SA =1

If ia > ia∗ switch 1 is turned OFF and switch 4 is turned ON SA = 0

If ib < ib∗ switch 3 is turned ON and switch 6 is turned OFF SB =1

If ib > ib∗ switch 3 is turned OFF and switch 6 is turned ON SB = 0

If ic < ic∗ switch 5 is turned ON and switch 2 is turned OFF SC =1

If ic > ic∗ switch 5 is turned OFF and switch 2 is turned ON SC = 0

3.2.6 Mathematical Model of Voltage Source Inverter (VSI)

In some simulation applications, mainly the voltage drops of the power electronic devices (e.g. IGBTs, Diodes etc.) are neglected due to its simplicity. Therefore, the performance of the control system obtained is not the same as the experimental results. Based on that we try to see model of both ideal and real inverter.

3.2.6.1 Model of Real Inverter

The power electronic devices (e.g. IGBTs, Diodes etc.) are nonlinear. It is well-known that the voltage drop of the power electronic devices causes distorted motor voltage and increasing motor current harmonic distortion, and reduction of the fundamental voltage/current component. This model includes the voltage drops in the IGBT switching devices and the freewheeling diodes which are shown in Fig 3.6. It is known that the instantaneous voltage drops of one converter leg presented by a switching device or a freewheeling diode can be represented by an on-state forward voltage drop connected in series with an on-state resistance. Thus, this voltage drop of one inverter leg can been calculated by Equation (3.13), (3.15)

$$v_{drop} = v_f + R_{on} i \tag{3.13}$$

where v_f is the on-state forward voltage drop and R_{on} is the on-state resistance. In addition, the inverter voltage drop on one inverter leg depends on both its instantaneous switching state and its relevant phase current direction (Song, 2020). There are four cases considered as follows:

Case 1: if the current i_{as} flows to load (i_{as} > 0) and the (S_1 =1) as shown in Fig. 3.5(a) then the terminal voltage v_{ao} is defined by can been calculated as

$$v_{ao} = V_{dc} - v_i = V_{dc} - v_{fi} - R_{oni} |i_{as}| \quad (3.14)$$

where V_i is the voltage drop of the IGBT; v_{fi} and R_{oni} are the forward drop of IGBT, on-state resistance of IGBT, respectively.

Case 2: if (i_{as} < 0) and the (S_1=1) as shown in Fig. 3.5(b) then the terminal voltage v_{ao} is defined by

$$v_{ao} = V_{dc} + v_d = V_{dc} - v_{fd} - R_{ond} |i_{as}| \quad (3.15)$$

Where v_d is the voltage drop of the Diode; v_{fd} and R_{ond} are the forward drop of Diode, on state resistance of Diode, respectively

Case 3: if the current i_{as} flows to load (i_{as}< 0) and the (S_1= 0) as shown in Fig. 3.5(c) then the terminal voltage v_{ao} is defined by

$$v_{ao} = v_i = V_{fi} + R_{oni} |i_{as}| \quad (3.16)$$

Case 4: if the current i_{as} flows to load (i_{as} > 0) and the (S_1=0) as shown in Fig. 3.5(d) then the terminal voltage v_{ao} is defined by

$$v_{ao} = -v_d = -v_{fi} + R_{oni} |i_{as}| \quad (3.17)$$

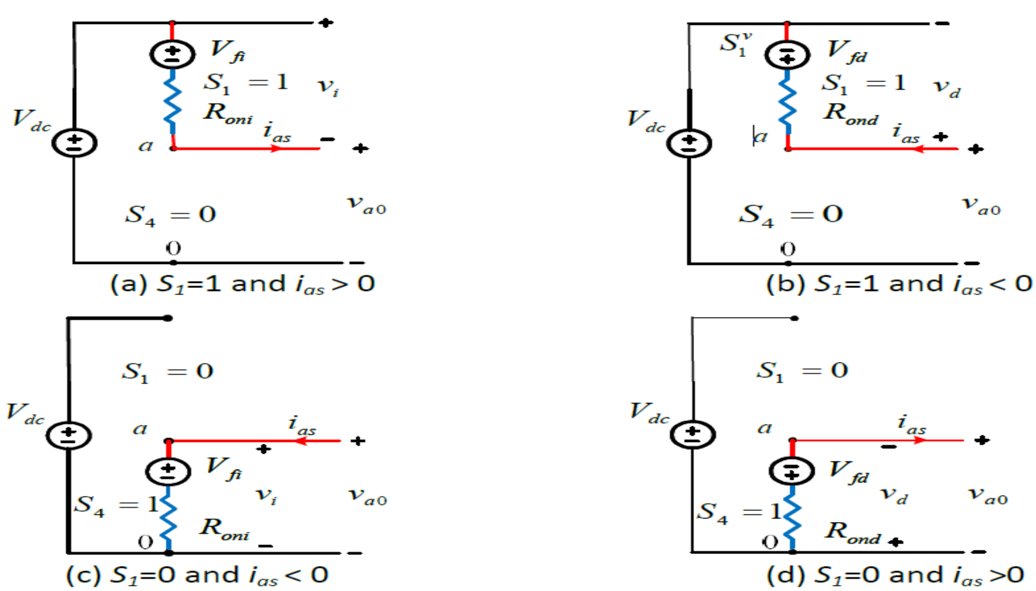

Figure 3.5 Voltage drop on one inverter leg

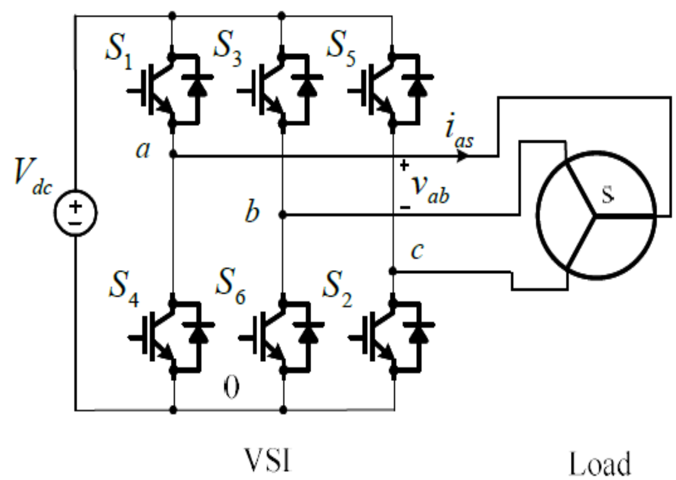

Figure 3.6 Model of Real Voltage Source Inverter (VSI) (Aka, 2023)

3.2.6.2 Model of an Idea Inverter

Fig. 3.7 shows an ideal two-level three-phase voltage source inverter (VSI) with six idealized switches, S_1 to S_6 and a dc constant voltage source V_{dc} connecting a three-phase load. This inverter having the power devices are considered as ideal switches which there are no snubbers and gate drive circuits. Each phase leg of the VSI is represented by a "switch" that has three input terminals as follow:

$$v_{as} = v_{a0} - v_{s0} \tag{3.18}$$

$$v_{bs} = v_{b0} - v_{s0} \tag{3.19}$$

$$v_{cs} = v_{c0} - v_{s0} \tag{3.20}$$

Where v_{as}, v_{bs} , and v_{cs} are the phase-to-neutral voltages.

$$v_{as} + v_{bs} + v_{cs} = v_{a0} + v_{b0} + v_{c0} - 3v_{s0} \tag{3.21}$$

Assuming that the system is balanced operation

$$v_{as} + v_{bs} + v_{cs} = 0 \tag{3.22}$$

$$v_{s0} = \frac{v_{a0} + v_{b0} + v_{c0}}{3} \tag{3.23}$$

$$v_{as} = \frac{2v_{a0} - v_{b0} - v_{c0}}{3} \tag{3.24}$$

Frequency of the inverter and the high torque ripple resulting from the use of flux and torque hysteresis controllers (Hussien, 2019, December).

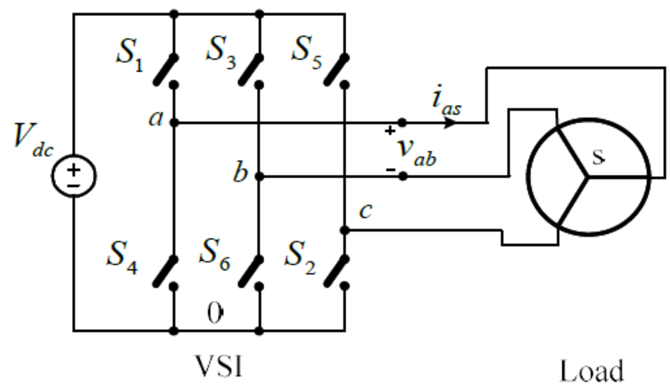

Figure 3.7 Ideal two-level three-phase voltage source inverter (VSI) (Almaktoof, 2014)

3.2.7 Field Oriented Control Methods

Knowledge of the instantaneous rotor flux position (angle), with which the revolving reference frame is aligned, constitutes the necessary requirement for proper transformation from stationary reference frame to rotating reference frame, or vice versa, in field orientation. In fact if there is an error in this variable, the d^e-axis is not aligned with the rotor flux vector. Thus, I_d^e and I_q^e are incorrect flux and torque components of the stator currents.

There are two general methods to measure the rotor flux vector angle. One, called the direct or feed-back method was invented by Blaschke, and the other, known as the indirect or feed-forward method was invented by Hasse. The two methods differ in the way the rotor angle is determined.

3.2.7.1 Direct Field Oriented Control

In direct field oriented control (DFOC), the angle and magnitude of the reference flux vector are either measured or estimated from the stator currents and voltage using flux observers. Figure 3.8 shows a simple scheme for estimation the magnitude and phase (position) of the rotor flux vector, based on measuring the air gap flux and stator current. Placing two Hall sensors of magnetic field in the air gap of the motor, allows determination of the direct and quadrature components, λdm and λqm, of the air gap flux vector, λm. In analytical form, the rotor flux vector can be expressed as

$$\lambda_r = \frac{L_r}{L_m}\lambda_m - L_{1r}I_s \quad (3.25)$$

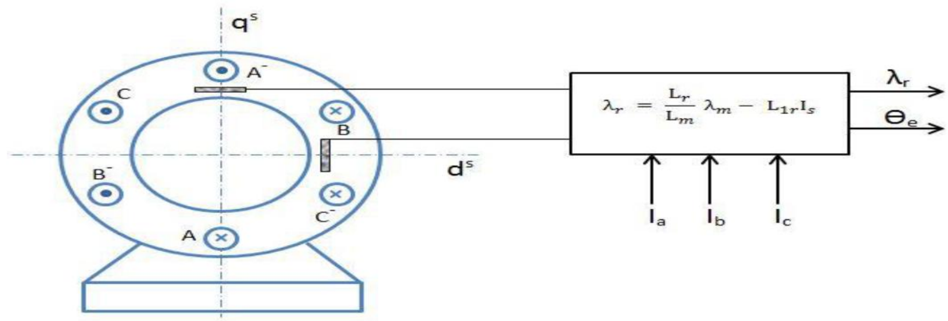

Figure 3.8 Magnitude and position of the rotor flux vector using Hall sensors and a rotor flux (Kapor.B, 2023)

Calculated using equation (3.25), signals λdr and λqr calculated as

$$\lambda_{dr} = \frac{L_r}{L_m}\lambda_{dm} - L_{1r}I_d^s \quad (3.26)$$

$$\lambda_{qr} = \frac{L_r}{L_m}\lambda_{qm} - L_{1r}I_q^s \quad (3.27)$$

Magnitude, λr, and phase, Θe, of the rotor flux vector are determined using the rectangular to polar coordinate transformation

$$\lambda_{dr} + j\lambda_{qr} \xrightarrow{yields} \lambda_r < \theta_e \quad (3.28)$$

Installing sensors in the air gap are inconvenient, and they spoil the ruggedness of the induction motor. Therefore, the stator current and voltage are using to compute the rotor flux vector. The stator flux vector can be estimated using following equation

$$\lambda_s = \int_0^t (\lambda_s - R_s I_s)dt + \lambda_s(0) \quad (3.29)$$

The air gap flux using the following equation

$$\lambda_m = \lambda_s - L_{1s} I_s \qquad (3.30)$$

And the rotor flux vector, λr, can be estimated from equation (3.8) (Aktas, 2020).

3.2.7.2 Indirect Field Oriented Control

Indirect field orientation (IFO) is an alternative approach to direct flux orientation. It is based on calculation of the slip speed ωr. The angular position, Θe, of the rotor flux vector is expressed as

$$\theta_e = \int_0^t \omega_{sl} dt + \omega_{act} dt \qquad (3.31)$$

Where ω_{act} is the rotor speed, which is easy to measure using a shaft position sensor. And ω_{sl} is the slip frequency speed. The required value of slip speed can be calculated by following equation

$$\omega_{sl} = \frac{L_m}{L_r} \cdot \frac{R_r}{\psi_r} \cdot I_q^e \qquad (3.32)$$

The IFO is more popular than DFO in industrial application due to implementation simplicity.

Indirect Field Oriented Control Algorithm

The block diagram of indirect field oriented control method is shown in figure 3.9. The induction motor is fed by a variable voltage, variable frequency PWM inverter, which operates in current control mode. The control scheme generates inverter switching commands to achieve the desired torque at the motor shaft. The algorithm of IFOC is given as:

i. Measure the stator phase currents *Ia*, *Ib*, and *Ic*. These currents are feed to Clarke transformation module that gives two components, I_d^s and I_q^s, in stationary reference frame.

ii. Transform the set of these two currents I_d^s and I_q^s, into rotating reference frame. This conversion called Park transformation, and provides I_d^e and I_q^e.

iii. The rotor flux is computed by

$$\psi_r = \frac{L_m I_d^e}{1+\tau_r} \tag{3.33}$$

Where τ_r is the rotor time constant calculated by

$$\tau_r = \frac{L_r}{R_r} \tag{3.34}$$

iv. The rotor angle, Θe, required for coordinate transformation is computed by equation (3.31).

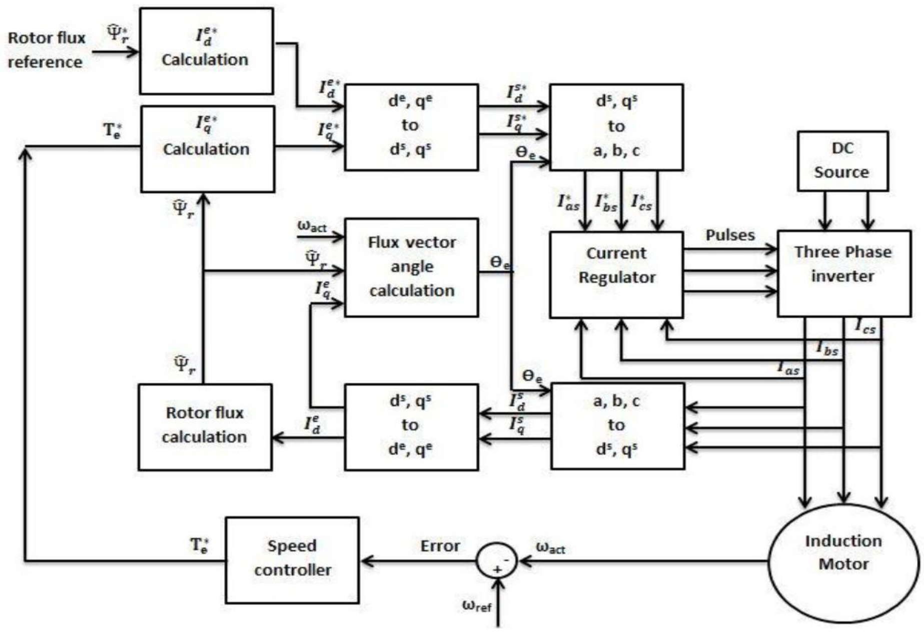

Figure 3.9 Indirect field oriented control scheme (Wang, 2018)

v. The motor speed which measured by encoder, ω_{act}, is compared with the reference speed ω_{ref} and the error produced is fed to the speed controller. The output of the speed controller is electromagnetic torque T_e^*.

vi. The quadrature stator current component reference I_q^{e*} is calculated by

$$I_q^{e*} = \left(\frac{2}{3}\right)\left(\frac{2}{p}\right)\left(\frac{L_r}{L_m}\right)\left(\frac{T_e^*}{\psi_r}\right) \tag{3.35}$$

vii. The direct stator current component reference I_d^{e*} is obtained by

$$I_d^{e*} = \frac{\psi_r^*}{I_m} \tag{3.36}$$

viii. I_d^e and I_q^e current references are converted into I_d^s and I_q^s, current references in stationary reference frame by using inverse Park transformation.

ix. I_d^s and I_q^s current references are converted into phase current references $Ia*$, $Ib*$, and Ic* by using inverse Clarke transformation and fed to the current controller. The controller processes the measured and reference currents to produce the inverter gating signals (Wang, 2018).

3.2.8 Controller Design

To obtain the required performance of an Induction motor drive system, these two control methods are integrated. The first technique is the LQR based current control, where the inner current loop can be optimized through optimal feedback gain. The optimal gain is usually based on minimization of cost function that contains states and inputs penalty cost. The second method is FLC, which uses IF-THEN rules to adjust the amplitude of the reference current online based on the speed error and change in speed error to accomplish the needed speed tracking. The fuzzy controller controls the outer speed loop of the motor drive system. The third technique is a combined form of fuzzy logic and LQR control techniques where both the inner current loop and outer speed loop are controlled simultaneously with FLC and LQR controller respectively.

3.2.8.1 LQR Controller design

In the closed-loop system, the linear quadratic regulator (LQR) is a common approach for calculating the state feedback gain. For a particular cost function weighting matrix, it is the optimum technique for relocating open-loop poles to produce a stable system with optimal control input utility and lowest cost. That is, when employing the optimum regulator approach, freedom of choice is lost for both discrete-time and continuous-time systems, because there are some locations where the poles cannot be assigned in order to get a positive-definite Riccatti equation solution. The control action is included in the cost function to keep the amount of energy used by the control action to a minimum. At its heart, the LQR algorithm is just an automated method of locating an appropriate state feedback controller.

In the design of a state-feedback control of an Induction motor system, the appropriate selection of a feedback system structure is critical. It is necessary to measure and use the state variables of the system to regulate the speed of the Induction motor. The state variables can be utilized to build a feedback controller if they are known. Figure 3.10 depicts the general structure of LQR controlled Induction motor drive system (Okyere E. B., 2019).

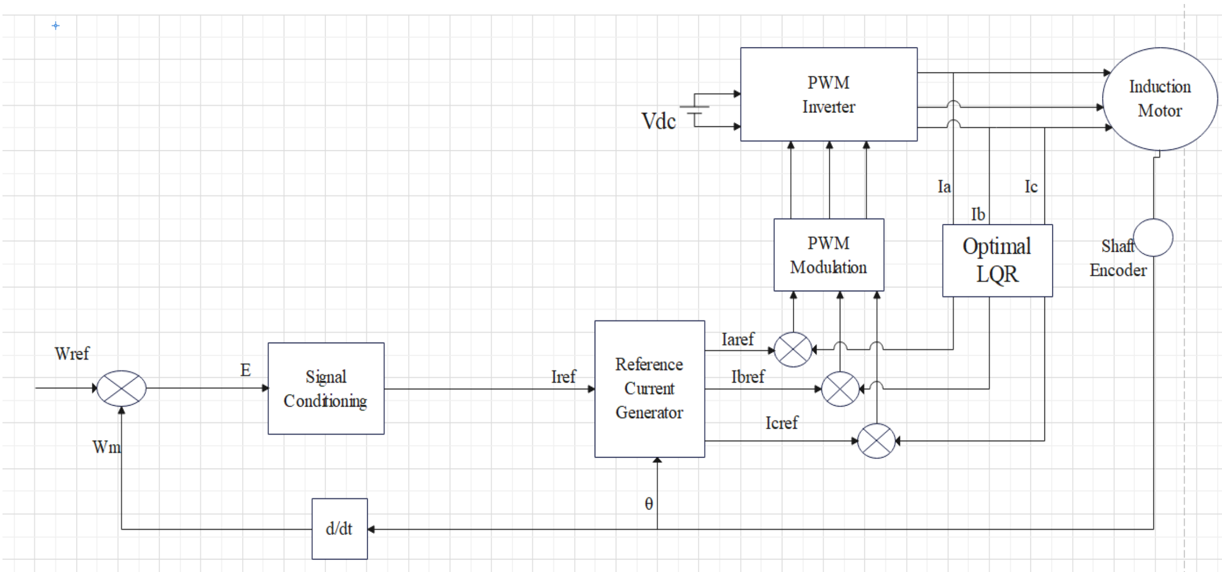

Figure 3.10 Block diagram of LQR controlled IM drive

The linear quadratic regulator was applied to the inner current loop so as to generate a control input that moves the states (*ia, ib,* and *ic*) along their optimal trajectory. The design of the controller is based on 3.5 of the inner loop variables (i.e. *ia, ib,* and *ic*). The differential Equation derived from eq(3.1-3.10)can be rewritten as:

$$\frac{d}{dt}\begin{bmatrix} i_{as} \\ i_{bs} \\ i_{cs} \end{bmatrix} = -\begin{bmatrix} \frac{R_s}{L-M} & 0 & 0 \\ 0 & \frac{R_s}{L-M} & 0 \\ 0 & 0 & \frac{R_s}{L-M} \end{bmatrix}\begin{bmatrix} i_{as} \\ i_{bs} \\ i_{cs} \end{bmatrix} + \begin{bmatrix} \frac{1}{L-M} & 0 & 0 \\ 0 & \frac{1}{L-M} & 0 \\ 0 & 0 & \frac{1}{L-M} \end{bmatrix}\begin{bmatrix} V_{as} \\ V_{bs} \\ V_{cs} \end{bmatrix} \quad (3.37a)$$

$$y = \begin{bmatrix} i_{as} \\ i_{bs} \\ i_{cs} \end{bmatrix} = \begin{bmatrix} 1 & 0 & 0 \\ 0 & 1 & 0 \\ 0 & 0 & 1 \end{bmatrix}\begin{bmatrix} i_{as} \\ i_{bs} \\ i_{cs} \end{bmatrix} \quad (3.37b)$$

Using the parameters in table 4.1, matrix A, B, C and D can be obtained as:

$$A = -\begin{bmatrix} \frac{R_s}{L-M} & 0 & 0 \\ 0 & \frac{R_s}{L-M} & 0 \\ 0 & 0 & \frac{R_s}{L-M} \end{bmatrix} \tag{3.37c}$$

$$B = \begin{bmatrix} \frac{1}{L-M} & 0 & 0 \\ 0 & \frac{1}{L-M} & 0 \\ 0 & 0 & \frac{1}{L-M} \end{bmatrix} \tag{3.37d}$$

$$C = \begin{bmatrix} 1 & 0 & 0 \\ 0 & 1 & 0 \\ 0 & 0 & 1 \end{bmatrix} \tag{3.37e}$$

$$D = \begin{bmatrix} 0 & 0 & 0 \\ 0 & 0 & 0 \\ 0 & 0 & 0 \end{bmatrix} \tag{3.37f}$$

Controllability test

Before the design process can begin, controllability matrices must be generated to determine whether an optimum controller exists for the system in consideration. For the above Induction motor system of Equation :

$$\dot{x} = Ax + Bu \tag{3.38a}$$

$$y = Cx + Du \tag{3.38b}$$

Where A, B, C, and D are the system matrix, input matrix, output matrix, and feed-forward matrix, respectively. x is the state vector, u is the control input vector, and Y is the output vector.

Definition 3.1 (Controllability) A system is completely controllable if there exists control input u(t) that can transfer any initial state of a system $x(t_0)$ to any other desired final state $x(t_f)$ within a finite time. Analytically for a linear system of the form of (3.38), controllability can be checked by computing the rank of the controllability matrix

$$Co = \left[B : AB : A^2 B : .... : A^{n-1} B \right] \tag{3.39}$$

If the rank of Co is equal to *n*, then the system is completely controllable.

From Equation (3.37), the controllability matrix is given by

$$C_o = 10^6 \times \begin{bmatrix} 0.002 & 0 & 0 & 0.0412 & 0 & 0 & 9.9156 & 0 & 0 \\ 0 & 0.002 & 0 & 0 & 0.0412 & 0 & 0 & 9.9156 & 0 \\ 0 & 0 & 0.002 & 0 & 0 & 0.0412 & 0 & 0 & 9.9156 \end{bmatrix} \tag{3.40}$$

Since the rank of C_o is 3, it is possible to design a state feedback controller.

Determination of the optimal gain matrix 'K_{opt}'

The goal of the LQR design is to find the control laws

$$u = -Kx \tag{3.41}$$

such that minimizes the quadratic cost function while driving the states along the desired trajectory. The cost optimization problem can be solved by substituting equation (3.41) into the state space equation (3.38a)

$$\dot{x} = (A - BK)x \tag{3.42}$$

And by introducing the following cost function:

$$J = \int_0^\infty \left[x^T Q x + u^T R u \right] dt, \tag{3.43}$$

Where Q and R are the state and input weighting matrices

Assuming the matrix $(A-BK)$ has Eigen values with negative real parts, the cost function becomes:

$$J = \int_0^\infty \left[x^T Q x + x^T K^T R K x \right] dt \tag{3.44}$$

$$J = \int_0^{\infty} \left[x^T (Q + K^T RK) x \right] dt \qquad (3.45)$$

Now let

$$-\frac{d}{dt}(x^T Px) = x^T (Q + K^T RK) x \qquad (3.46)$$

Where *P* is a positive definite Hermitian or real symmetric matrix then the derivation for *P* is as follows:

$$-\frac{d}{dt}(x^T Px) = -x^T Px - x^T P\dot{x}$$

$$= -[(A - BK)x]^T Px + x^T P(A - BK)x$$

$$= -x^T (A^T P - K^T B^T P + PA - PBK)x \qquad (3.47)$$

Comparing Equations (3.47) and (3.48) and noting that the equation must hold for any x, it requires that:

$$A^T P - K^T B^T P + PA - PBK = -(Q + K^T RK) \qquad (3.48)$$

The *Q* and *R* element compositions have a significant impact on system performance. The quadratic performance index is simply a weighted integral of the states and inputs when the weighting matrices are chosen as diagonal matrices.

By observing *Q* as state error penalty and *R* as penalty on control input, these weighting matrices are regarded the tuning parameters of LQR. The number of state and input variables determines the size of *Q* and *R* matrices, respectively. *Q* should be a positive semi-definite matrix and R should be a positive definite matrix for the LQR to give a stable response. According to Hamilton-Jacobi equation, the optimal gain matrix *K* can be given as:

$$K = R^{-1} B^T P \qquad (3.49)$$

Where *'P'* is a positive definite Hermitian or real symmetric matrix.
Now substituting equation (3.49) into equation (3.48), we arrive at an algebraic Riccati equation as follows:

$$PA + A^T P + Q - PBR^{-1} B^T P = 0 \qquad (3.50)$$

The positive definite matrix *'P'* can be obtained by solving equation (3.50) which is the used to determine the optimal control law

$$u(t) = -Kx(t) = -R^{-1}B^{T}Px(t) \tag{3.51}$$

The state variables (i_a , i_b and i_c) of the inner loop system were feedback through the Optimal gain matrix *K*. This Optimal gain matrix is calculated based on minimization of quadratic cost function. The aim is to generate a control input that will drive the actual states (i_a , i_b and i_c) to track desired states along the optimal trajectory (Okyere E. B., 2019).

Choosing of weighting matrices *R* and *Q*

The *Q* and R element compositions have a significant impact on system performance. The cost function is reduced to a quadratic term when the penalty matrices *Q* and *R* are chosen as diagonal matrices, which simplifies the optimization issue.
Therefore, the state weighting matrix *Q* and input weighting matrix *R* can be selected by trial and error which gives as optimal result as follow:

$$Q = w_Q C^T C \tag{3.52}$$

$$R = w_R I_{3x3} \tag{3.53}$$

The state feedback gain vector (*K*) of the LQR controller can then be calculated using the solution of algebraic Riccati equation (matrix *P*) of Equation (3.50). The solution of Equation (3.54) will be:

$$P = \begin{bmatrix} 0.0165 & 0 & 0 \\ 0 & 0.0165 & 0 \\ 0 & 0 & 0.0165 \end{bmatrix} \tag{3.54}$$

And an Optimal gain matrix *K* can be calculated as follow:

$$K = R^{-1}B^{T}P \tag{3.55}$$

3.2.8.2 FLC controller design

FLC is a control algorithm that is based on a linguistic control strategy that is converted into an automated control strategy using expert knowledge. A FLC's functioning is based on qualitative understanding about the system under control.

Instead of using mathematical equations, fuzzy logic uses linguistic terms to express operational rules. Many systems are highly complicated to represent them correctly, even using complex mathematical expressions. As a result, old approaches are no longer viable. Fuzzy logic linguistic terms, on the other hand, provide a viable method for defining the operational characteristics of such a system and even perform well with only approximate data (Bernal, 2021).

FLC was chosen in this study for a variety of reasons.

- ✓ Designing without understanding the accurate model of the process is possible.
- ✓ Control simplicity and smooth functioning.
- ✓ Tolerance is quite high.
- ✓ The price is low.
- ✓ Non-linearity's influence is reduced.
- ✓ Approximation ability is inherent in the system.

The FLC controller is made up of three major parts.

- ➢ Fuzzification
- ➢ Fuzzy inference
- ➢ Defuzzification

Fuzzification: Fuzzification is the process of converting a crisp input into a fuzzy set.

The following functions will be performed in this step:

i. Multiple measured crisp inputs first must be mapped into fuzzy membership function this process is called fuzzification.

ii. Performs a scale mapping to convert the range of input variable values into corresponding discourse universes.

iii. Performs the function of fuzzification by converting input data into suitable linguistic variables which may be viewed as labels of fuzzy sets. Logic implications, such as if-then rules, are frequently used to convey fuzzy logic language words. Fuzzy membership functions are defined by rules as a set of values. A triangular, trapezoidal, bell (as illustrated in Fig.3.11), or other suitable form can be used to represent a fuzzy membership function (Jung, 2019, August)).

The triangular membership functions limits are defined by three values *Val1*, *Val2* and *Val3*.

$$\mu(u_i) = \left.\begin{array}{l} \dfrac{u_i - V_{al1}}{V_{al2} - V_{al1}}, V_{al1} \le u_i \le V_{al2} \\ \dfrac{V_{al3} - u_i}{V_{al3} - V_{al2}}, V_{al2} \le u_i \le V_{al3} \\ 0, \quad Otherwise \end{array}\right\} \tag{3.56}$$

The trapezoidal membership functions are limited by four values Val1, Val2, Val3 and Val4.

$$\mu(u_i) = \left.\begin{array}{l} \dfrac{u_i - V_{al1}}{V_{al2} - V_{al1}}, V_{al1} \le u_i \le V_{al2} \\ \quad 1 \quad , V_{al2} \le u_i \le V_{al3} \\ \dfrac{V_{al4} - u_i}{V_{al4} - V_{al3}}, V_{al3} \le u_i \le V_{al4} \\ 0, \quad Otherwise \end{array}\right\} \tag{3.57}$$

The bell-type membership functions limits are defined by parameters Xp, w and m as follows:

$$\mu(u_i) = \frac{1}{(1 + (\frac{|u_i - x_p|}{w}^{2m}))} \tag{3.58}$$

Where *Xp* is the midpoint and *w* is the width of bell function, m ≥1, and describe the convexity of the bell function

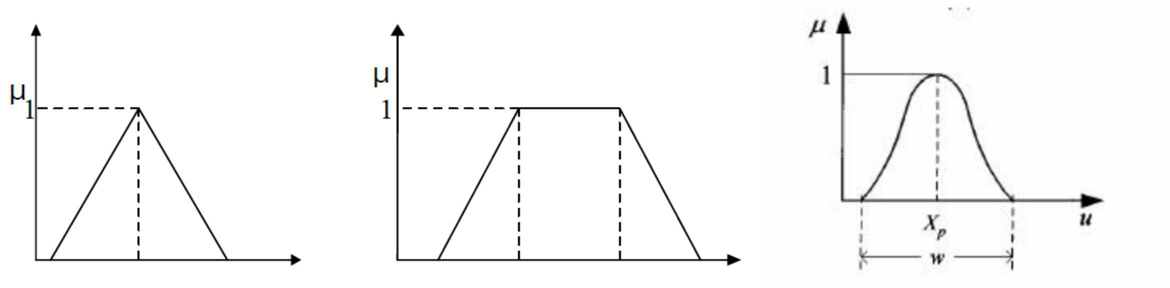

Figure 3.11 [a] Triangular MF, [b] Trapezoidal and [c] Bell membership function (Nik Badrul Alam, 2021)

The triangular membership function is the most utilized one in FLC designs since it is simple to convey the designer's idea and requires little computational effort. As a result, it is also utilized in this study.

The fuzzy controller's inputs are represented on various levels. Extremely large (EL), Very large (VL), Large (L), Medium (MM), Small (SS), Very small (VS), Extremely small (ES), or other levels can be defined as illustrated in Figure 3.12 A fuzzy set is used to describe each level (Nik Badrul Alam, 2021).

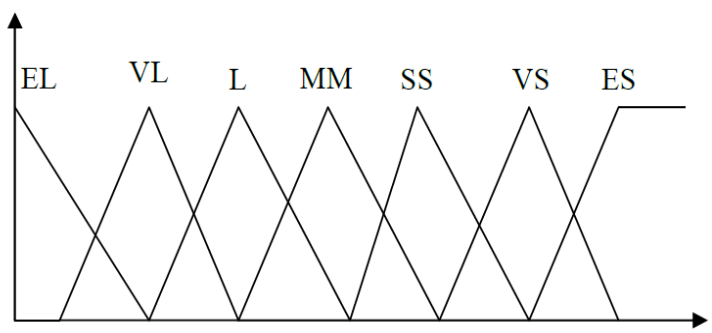

Figure 3.12 Structure of fuzzy membership function (Nik Badrul Alam, 2021)

Fuzzy inference system

The FLC second phase is fuzzy inference, which contains the knowledge base and decision-making logic. The knowledge base is made up of the rule base and the database. The description of the input and output variables is stored in the database. The control rules are evaluated by the decision-making logic. The control-rule basis may be built to relate the controller's output action to the acquired inputs.

The inference system determines which control rules are applicable at this time and then determines what the plant's input should be. The Mamdani model, the Sugeno model, and the

Tsukamoto model are the three main forms of fuzzy inference systems. The Mamdani "max and min" model is the most desirable of the three and is utilized in this study (Karaboga, 2019).

Defuzzification

Defuzzification is the process of converting a fuzzy output back into a crisp value. There are several methods which includes

i. **The Center of Gravity (COG) method**: COG is the widely used method. The centroid strategy generates the center of gravity of area bounded by the Membership function curve.

$$\bar{y} = \frac{\int \mu_Y(y) \cdot y dy}{\int \mu_Y(y) dy} \tag{3.59}$$

COG defuzzification technique is chosen in this study because it is fast and uses simple operations, and it offers a continuous change in defuzzification value, making it suitable for use in fuzzy controllers (Samavat, 2023).

Fuzzy based speed control of the drive system

The techniques for designing a fuzzy based speed controller are as follows:

i. Determine fuzzy variables based on the controller inputs and outputs.
ii. Separate the inputs and outputs into distinct fuzzy sets and name them according to the task at hand.
iii. For each fuzzy set, assign a membership function (MF) and fuzzify.
iv. Create a set of fuzzy IF-THEN rules, to address the problem.
v. Select the inference engine method which is Mamdani for this case.
vi. Add the fuzzy outputs of each rule together.
vii. Finally, to defuzzify the output, select a defuzzification technique (Farah, (2019)).

In the drive system there are two input variables, the speed error (e) and change in speed error (ce)

$$\text{Error: } e(k) = \omega_{ref}(k) - \omega_m(k) \tag{3.60}$$

$$\text{Change in error: } ce = e(k) - e(k\text{-}1) \tag{3.61}$$

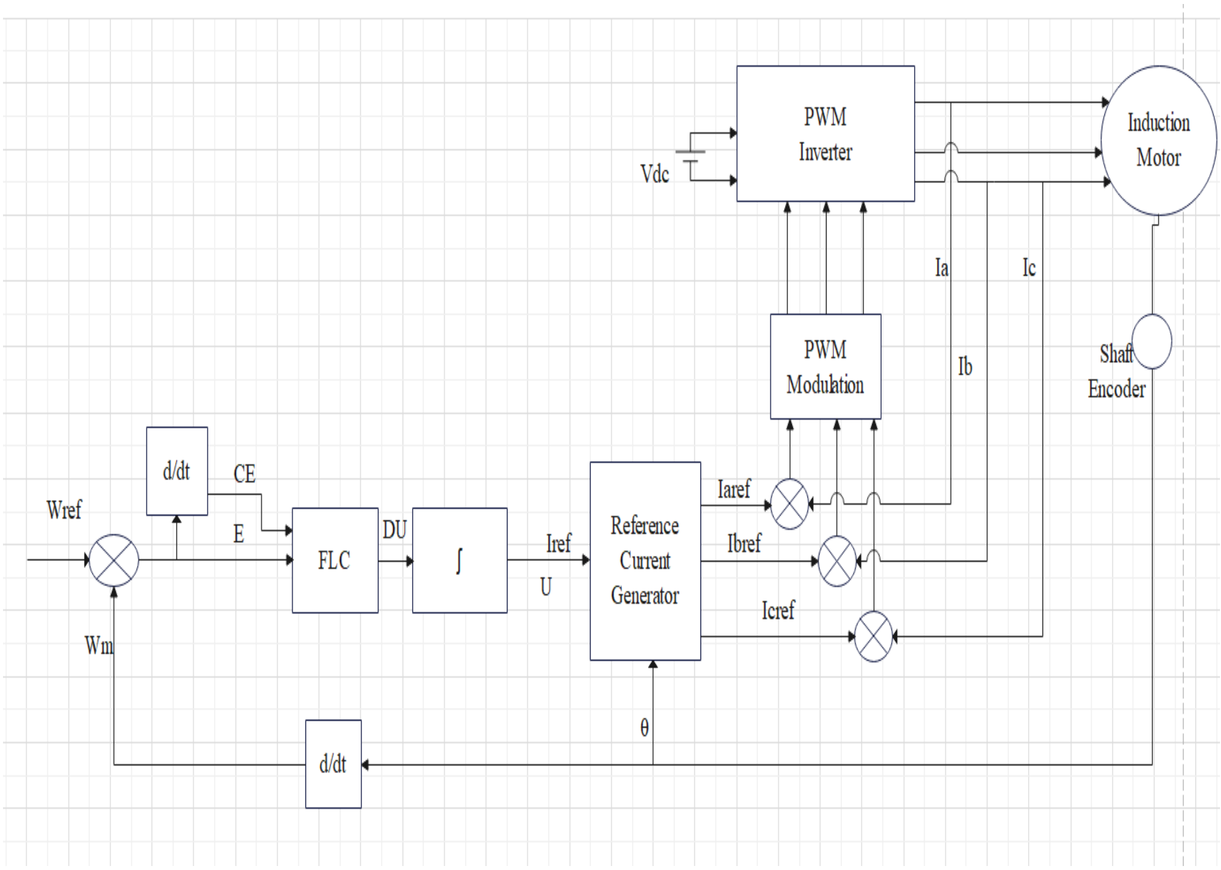

Figure 3.13 Fuzzy logic speed control of Induction motor

Input scaling factors G_e and G_{ce} map these two inputs into the corresponding normalized range as

$$\text{Normalized error: } E(k) = G_e e(k) \tag{3.62}$$

$$\text{Change in error: } CE(k) = G_{ce} ce(k) \tag{3.63}$$

When the inference engine infers the fuzzy output, the output is computed to provide the real control signal as

$$u = G_u U + G_i \int U dt \tag{3.64}$$

Where G_u and G_i are the output scaling factors.

The input and output scaling factors are obtained through trial and error since fuzzy logic itself needs only approximate data to perform well. The controller analyzes the speed error signal's pattern and updates the output accordingly, ensuring that the real speed Nact matches the desired speed Nref. The following is the fuzzy membership function for the input and output variables:

Table 3.2 Fuzzy membership functions and their symbols

Fuzzy membership functions	Symbols
Negative Big	NB
Negative Medium	NM
Negative Small	NS
Zero	ZE
Positive Small	PS
Positive Medium	PM
Positive Big	PB

The membership function for the speed error, the change in speed error and the change in reference current (control input) are shown in Figures 3.14 through 3.16. For all the three variables, membership functions of seven level fuzzy variables are used. Table 3.3 shows the 7 × 7 rule base table that was used in the proposed system.

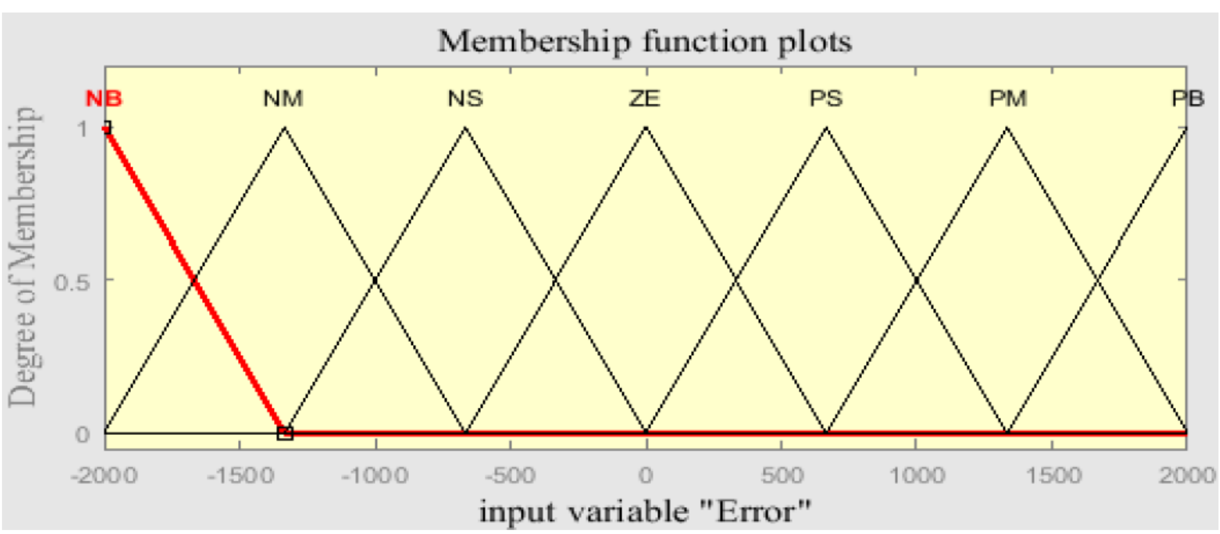

Figure 3.14 Membership function plot for input variable "Error"

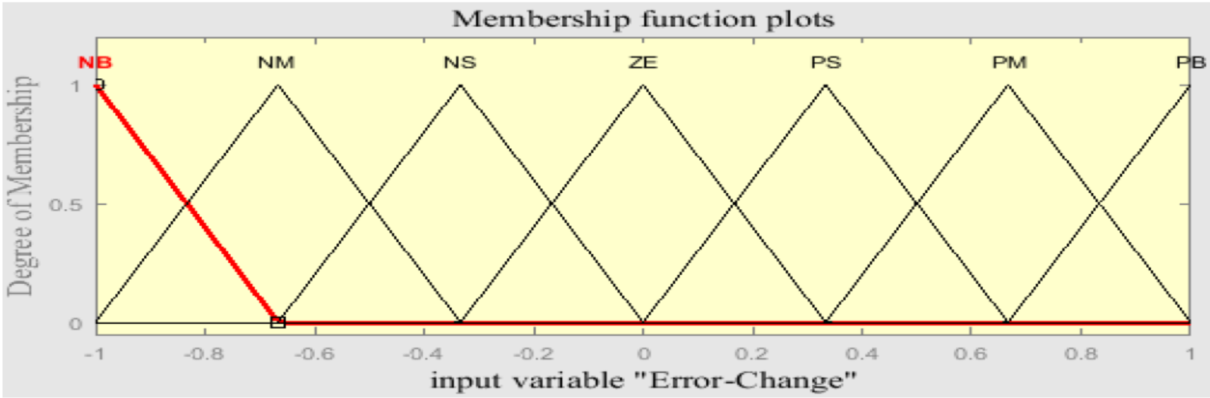

Figure 3.15 Membership function plot for input variable "Error Change"

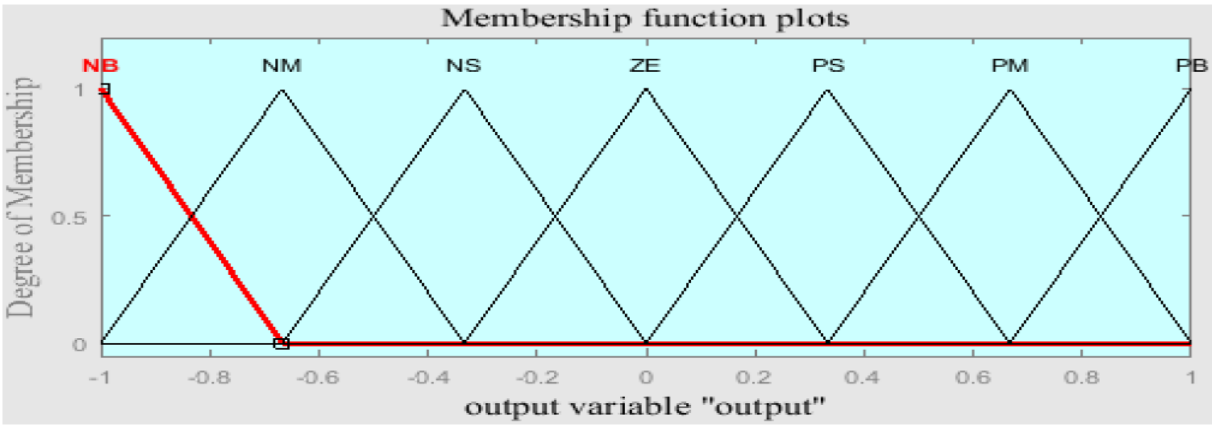

Figure 3.16 Membership function plot for output variable "Output"

Table 3.3 Rule base table for the drive system

E/CE	NB	NM	NS	ZE	PS	PM	PB
NB	NB	NB	NB	NB	NM	NS	ZE
NM	NB	NB	NB	NM	NS	ZE	PS
NS	NB	NB	NM	NS	ZE	PS	PM
ZE	NB	NM	NS	ZE	PS	PM	PB
PS	NM	NS	ZE	PS	PM	PB	PB
PM	NS	ZE	PS	PM	PB	PB	PB
PB	ZE	PS	PM	PB	PB	PB	PB

The universe of discourse of input parameters "Error" and "Error Change" is in the range -2000 to 2000 and -1 to 1 respectively. They can be fuzzified into seven triangular linguistic variables, as illustrated in Figures 3.14 and 3.15. The range of discourse for the output parameter "reference current" can be standardized to -1 to 1. It's also fuzzified into seven triangular membership functions as illustrated in Figure 3.16.

Rule base (decision making)

After we have established the input and output variables, as well as the MF, we will need to create the rule-base, which will be made up of expert IF <antecedents> and THEN <consequent> rules. These rules convert the input variables into an output that tells us how fast the motor will run. We have 49 rules depending on the number of MF for input and output variables. Figure 3.17 depicts the system's fuzzy inference system block.

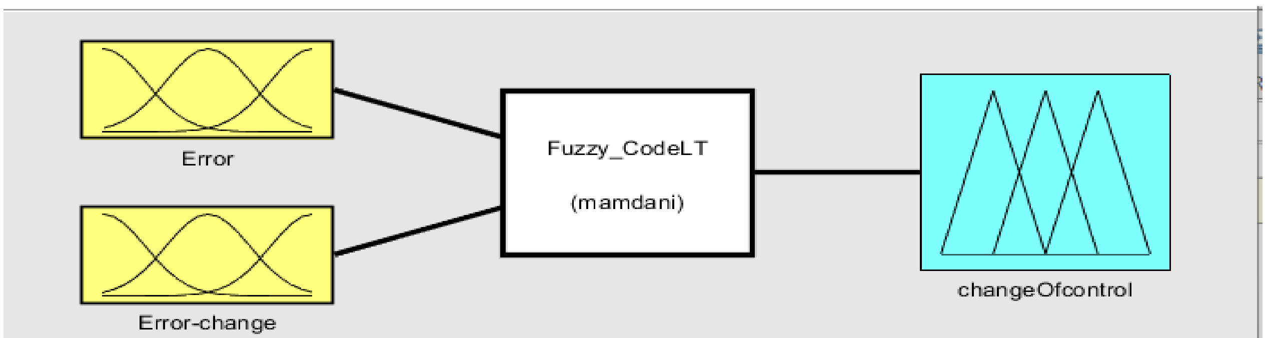

Figure 3.17 The system's fuzzy inference system

Here in this study the rules were derived based on the generated error and error change. The rules, the surface view, and rule view used in the proposed Fuzzy-LQR system are shown on Figure 3.18 through 3.20.

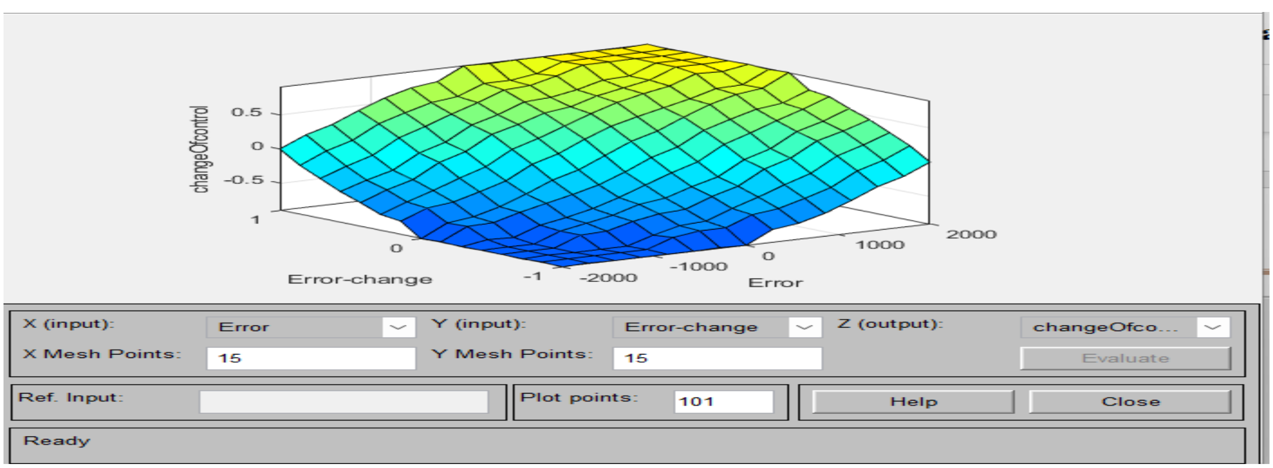

Figure 3.18 Surface view of the generated rules

1. If (Error is NB) and (Error-change is NB) then (changeOfcontrol is NB) (1)
2. If (Error is NB) and (Error-change is NM) then (changeOfcontrol is NB) (1)
3. If (Error is NB) and (Error-change is NS) then (changeOfcontrol is NB) (1)
4. If (Error is NB) and (Error-change is ZE) then (changeOfcontrol is NB) (1)
5. If (Error is NB) and (Error-change is PS) then (changeOfcontrol is NM) (1)
6. If (Error is NB) and (Error-change is PM) then (changeOfcontrol is NS) (1)
7. If (Error is NB) and (Error-change is PB) then (changeOfcontrol is ZE) (1)
8. If (Error is NM) and (Error-change is NB) then (changeOfcontrol is NB) (1)
9. If (Error is NM) and (Error-change is NM) then (changeOfcontrol is NB) (1)
10. If (Error is NM) and (Error-change is NS) then (changeOfcontrol is NB) (1)
11. If (Error is NM) and (Error-change is ZE) then (changeOfcontrol is NM) (1)
12. If (Error is NM) and (Error-change is PS) then (changeOfcontrol is NS) (1)
13. If (Error is NM) and (Error-change is PM) then (changeOfcontrol is ZE) (1)
14. If (Error is NM) and (Error-change is PB) then (changeOfcontrol is PS) (1)
15. If (Error is NS) and (Error-change is NB) then (changeOfcontrol is NB) (1)
16. If (Error is NS) and (Error-change is NM) then (changeOfcontrol is NB) (1)
17. If (Error is NS) and (Error-change is NS) then (changeOfcontrol is NM) (1)
18. If (Error is NS) and (Error-change is ZE) then (changeOfcontrol is NS) (1)
19. If (Error is NS) and (Error-change is PS) then (changeOfcontrol is ZE) (1)
20. If (Error is NS) and (Error-change is PM) then (changeOfcontrol is PS) (1)
21. If (Error is NS) and (Error-change is PB) then (changeOfcontrol is PM) (1)
22. If (Error is ZE) and (Error-change is NB) then (changeOfcontrol is NB) (1)
23. If (Error is ZE) and (Error-change is NM) then (changeOfcontrol is NM) (1)
24. If (Error is ZE) and (Error-change is NS) then (changeOfcontrol is NS) (1)
25. If (Error is ZE) and (Error-change is ZE) then (changeOfcontrol is ZE) (1)
26. If (Error is ZE) and (Error-change is PS) then (changeOfcontrol is PS) (1)
27. If (Error is ZE) and (Error-change is PM) then (changeOfcontrol is PM) (1)
28. If (Error is ZE) and (Error-change is PB) then (changeOfcontrol is PB) (1)
29. If (Error is PS) and (Error-change is NB) then (changeOfcontrol is NM) (1)
30. If (Error is PS) and (Error-change is NM) then (changeOfcontrol is NS) (1)
31. If (Error is PS) and (Error-change is NS) then (changeOfcontrol is ZE) (1)
32. If (Error is PS) and (Error-change is ZE) then (changeOfcontrol is PS) (1)
33. If (Error is PS) and (Error-change is PS) then (changeOfcontrol is PM) (1)
34. If (Error is PS) and (Error-change is PM) then (changeOfcontrol is PB) (1)
35. If (Error is PS) and (Error-change is PB) then (changeOfcontrol is PB) (1)
36. If (Error is PM) and (Error-change is NB) then (changeOfcontrol is NS) (1)
37. If (Error is PM) and (Error-change is NM) then (changeOfcontrol is ZE) (1)
38. If (Error is PM) and (Error-change is NS) then (changeOfcontrol is PS) (1)
39. If (Error is PM) and (Error-change is ZE) then (changeOfcontrol is PM) (1)
40. If (Error is PM) and (Error-change is PS) then (changeOfcontrol is PB) (1)
41. If (Error is PM) and (Error-change is PM) then (changeOfcontrol is PB) (1)
42. If (Error is PM) and (Error-change is PB) then (changeOfcontrol is PB) (1)
43. If (Error is PB) and (Error-change is NB) then (changeOfcontrol is ZE) (1)
44. If (Error is PB) and (Error-change is NM) then (changeOfcontrol is PS) (1)
45. If (Error is PB) and (Error-change is NS) then (changeOfcontrol is PM) (1)
46. If (Error is PB) and (Error-change is ZE) then (changeOfcontrol is PB) (1)
47. If (Error is PB) and (Error-change is PS) then (changeOfcontrol is PB) (1)
48. If (Error is PB) and (Error-change is PM) then (changeOfcontrol is PB) (1)
49. If (Error is PB) and (Error-change is PB) then (changeOfcontrol is PB) (1)

Figure 3.19 Generated rules using the two inputs and an output

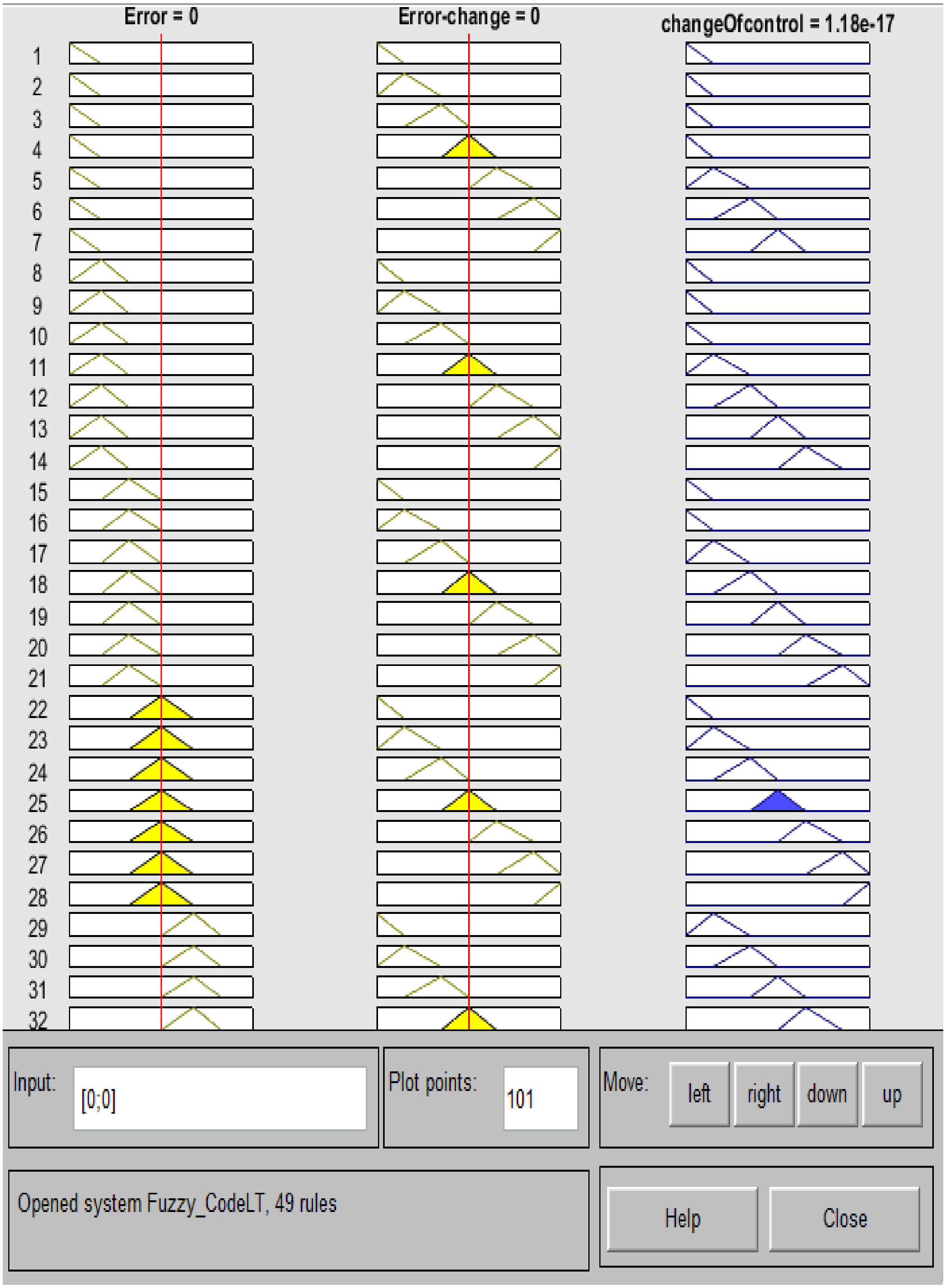

Figure 3.20 Rule view of the generated rules

CHAPTER FOUR

RESULTS AND DISCUSSIONS

4.1 Introduction

The MATLAB simulations, results, and discussion of the drive system are covered in this chapter. It is focused on the simulation findings of LQR, Fuzzy logic, and a combined Fuzzy-LQR controller for closed loop control of the drive system. The simulation is examined using the MATLAB/SIMULINK software package for step response, disturbance rejection, and model error of the closed loop system. The mathematical model of all the drive components are modeled using the Simulink blocks for simulation purpose. The Simulink model discussed here is used to run simulations and assess the performance of controllers at various operating speeds and control methods.

4.2 Simulink Model of the Drive System

The Induction motor model can be built utilizing the machine's voltage equations, electromechanical torque equation, and the current equation derived in chapter three. The block diagram has been created and simulated with a variety of solvers. These solve their respective Ordinary Differential Equations to compute the internal state variables. To see the features and the suitable model of the motor, a Simulink model of the motor and its drive is developed using MATLAB Simulink. Figure 4.1 depicts the entire Simulink model of the Induction motor driving system. The Induction motor drive Simulink model may be broken down into five basic blocks.

i. Induction Motor model

ii. Voltage source inverter blocks

iii. Switching pulse generator block (the six-step pulse generator)

iv. The reference current generator block

v. The controller block

Table 4.1 Lists the Induction motor parameters

Symbol	Description	Value	Unit
Rs	Per phase resistance	1.405	Ohm
L	Per phase inductance	0.178039	H
M	Mutual Inductance	0.1722	H
J	Equivalent Rotational inertia on the shaft	0.0131	Kg.m^2
K_t	Torque constant	1.4	N.m/A
P	Number of pole pairs	4	Pole pairs
Vdc	DC voltage source	200	Volt
$Nrated$	Rated Speed	1500	RPM
P	Rated power	30	Kw
I	Rated current	20	A

Figure 4.1 depicts the general block diagram of fuzzy-LQR controlled Induction motor drive system from which the overall Simulink diagram derived.

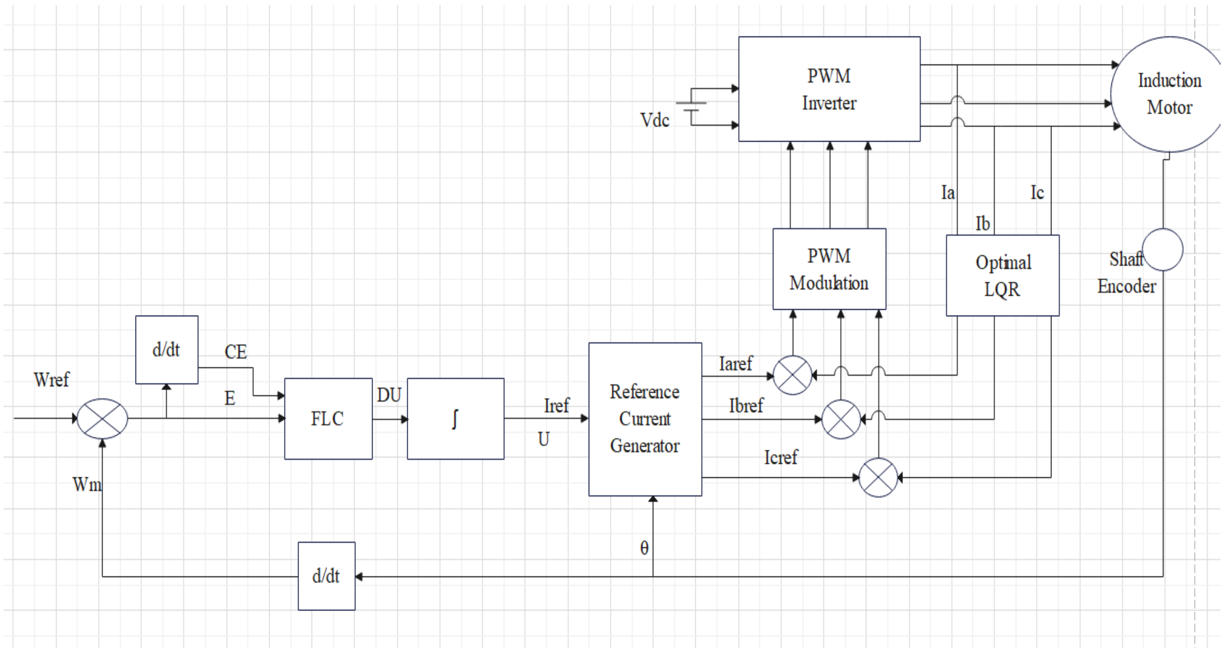

Figure 4.1 The general structure of fuzzy-LQR controlled Induction motor drive

4.2.1 Voltage equation model

Figure 4.2 shows the Simulink model for the voltage equation developed in Chapter three, Equation (3.7). The three phase stator current will be generated using torque load and the voltage from the three phase PWM inverter.

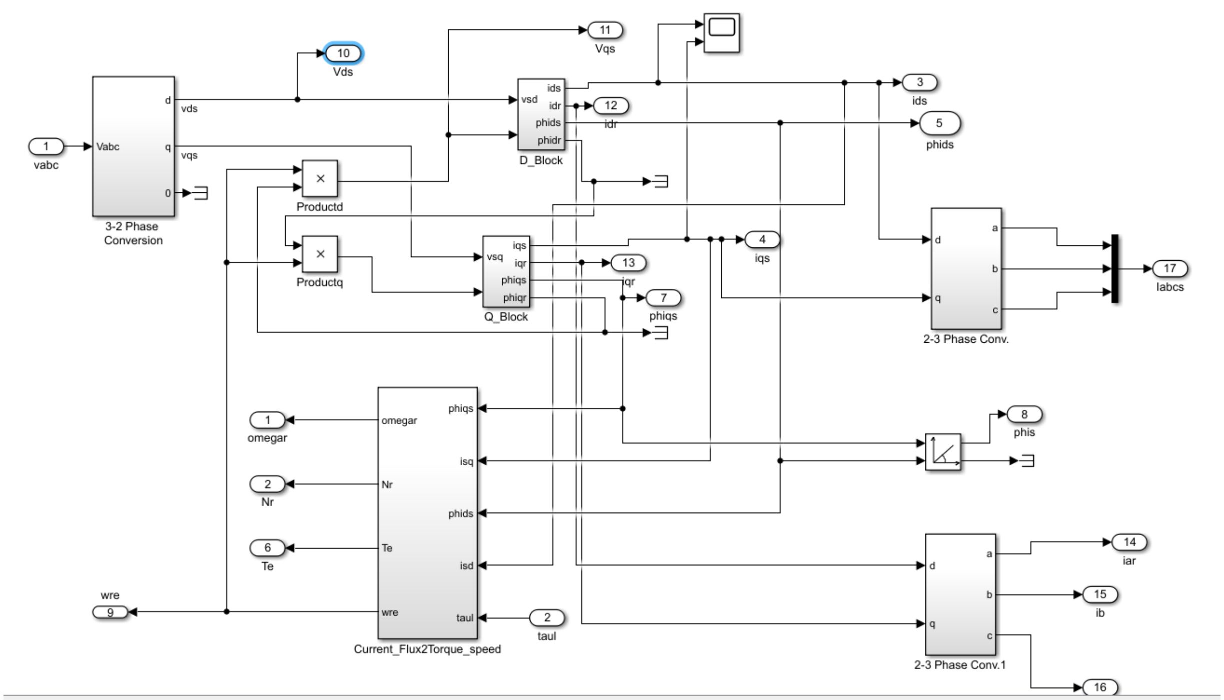

Figure 4.2 Voltage equation

4.2.2 Commutation Logic Model

The Induction motor's speed and torque are controlled by an electronic commutation mechanism in the drive system. The feedback from the motor's rotor position determines the order in which gate signals are distributed. Every 60 electrical degrees, the location of the motor is detected. Six switches pulses are created and utilized to control the Induction motor based on the position of the rotor. Using zero crossing error detection methods, the commutation sequence is created.

The commutation logic, which controls the inverter switches, is created once the position signals are determined. This model can produce a precise square wave switching pattern. Thus, generating signals for 6 switches. The three switching pulses generated are directly connected to the upper switches and not gate is used to switch the respective lower switches on the same leg. Figure 4.3 shows the Simulink model of the logic.

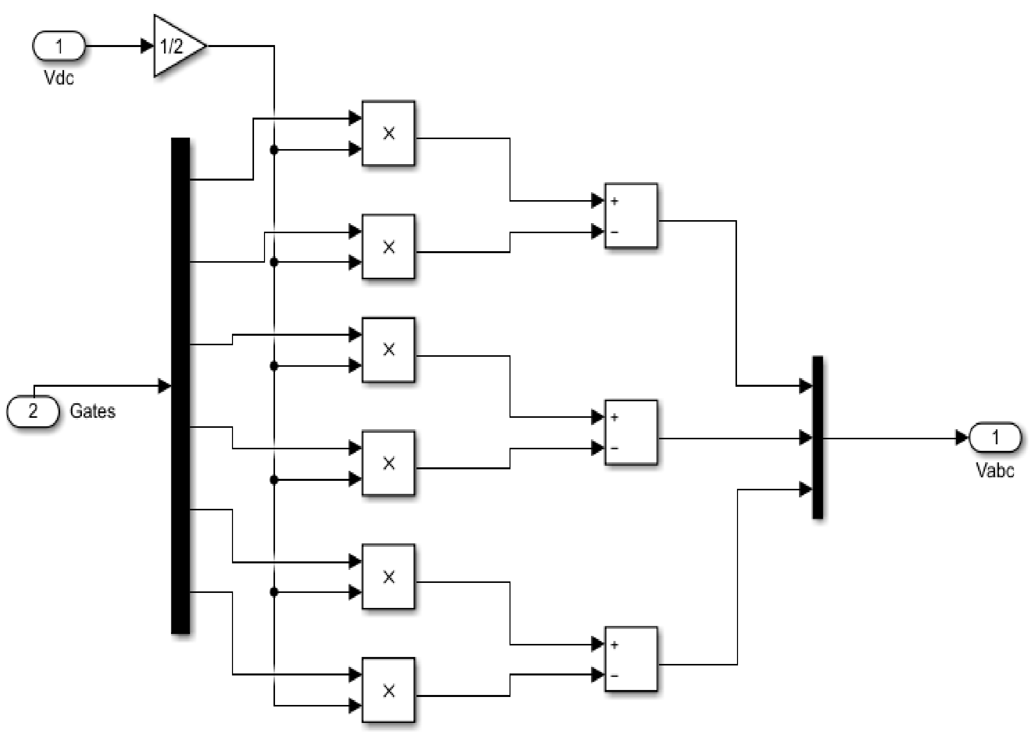

Figure 4.3 Inverter function model

4.2.3 Field Oriented Control Sub-Blocks

Indirect field oriented control algorithm has been simulated in MATLAB as shown in figure 4.4. All sub blocks will be reviewed in the next coming sections.

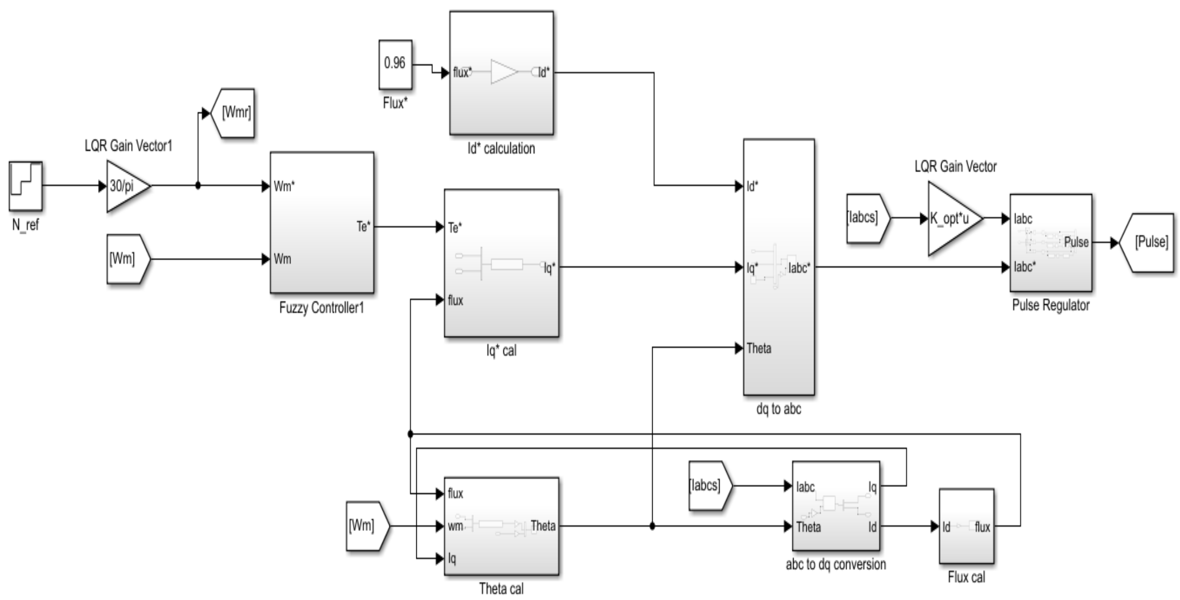

Figure 4.4 Field oriented control SIMULINK model

4.2.3.1 Forward Clarke and Park Transformation

Figure 4.4 shows the SIMULINK model that converts the *Ias, Ibs,* and *Ics* phase variables into I_d^e and $I_q^e$and current components in rotating reference frame *de-qe*. Equations (3.31) and (3.33) represent the mathematical relationship between the three-phase variables *Ias, Ibs,* and *Ics* and current components and I_d^e and I_q^e. The simulation is done by entering stator currents to the mux and applying the mathematical operation using function block parameters provided by MATLAB.

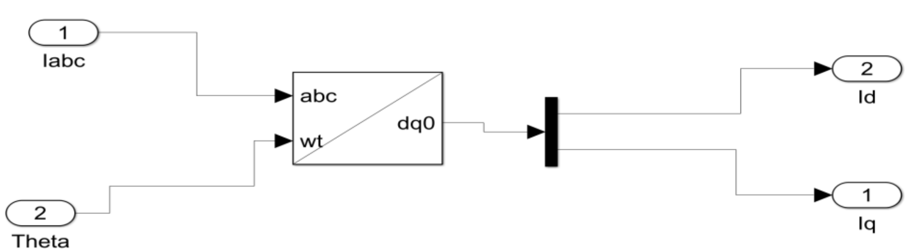

Figure 4.5 Field oriented control SIMULINK model

In figure 4.5, we define the following: *Θe* represents the angle between de-axis and rotor flux vector. *Iabc* represents the three-phase stator currents *Ias*, *Ibs*, and *Ics*. and I_d^e and I_q^e represents the stator current components in rotating reference frame.

4.2.3.2 Rotor Flux and Angle Calculation

Knowledge of the rotor flux vector magnitude and position is key information for field oriented control of the three-phase induction motor. The SIMULINK model of equations (3.33) and (3.31) are shown in figure 4.6 and 4.7 respectively.

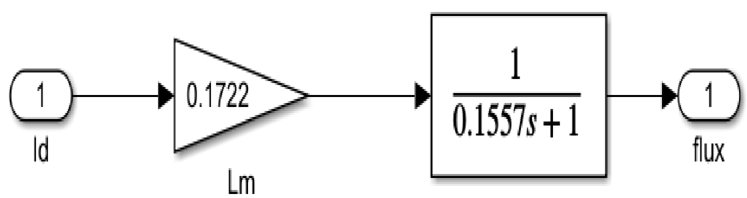

Figure 4.6 Rotor flux magnitude calculation

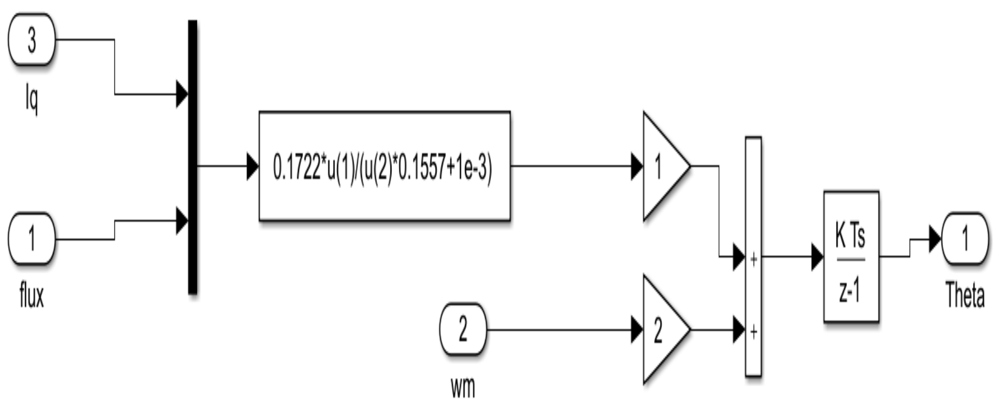

Figure 4.7 Theta calculation

SIMULINK model to calculate rotor flux position (angle) that is necessary for transformation from stationary to rotating reference frame or vice versa.

4.2.3.3 Direct Reference Current Calculation

The stator direct-axis current reference I_d^{e*} can be obtained using equation (2.22). Figure 4.6 shows the SIMULINK model of the two equations.

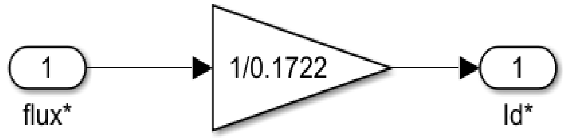

Figure 4.8 SIMULINK model to calculate the direct current reference component $\boldsymbol{I_d^{e*}}$

In figure 4.8, we have ψ^* represents the reference flux value. I_d^{e*} represents direct current reference component.

4.2.3.4 Quadrature Reference Current Calculation

The SIMULINK model shown in figure 4.6 used to obtain the stator quadrature reference current by using I_q^{e*} equations (3.33) and (3.35).

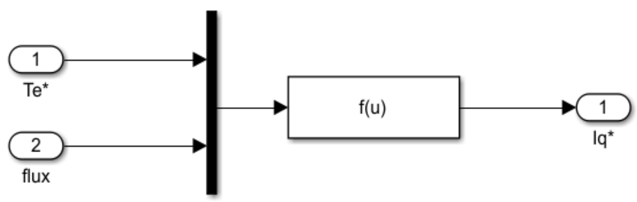

Figure 4.9 SIMULINK model to calculate quadrature current reference component $\boldsymbol{I_q^{e*}}$

In figure 4.9, we have T_e^* represents the reference torque obtained from speed controller. I_q^{e*} represents the quadrature reference current component.

4.2.3.4 Inverse Clarke and Park Transformation

The inverse transformation SIMULINK model is shown in figure 4.5. This block uses equations (3.4) to perform the conversion of I_d^e and I_q^e stator current components in rotating reference frame back *Ias*, *Ibs*, and *Ics* in stationary reference frame.

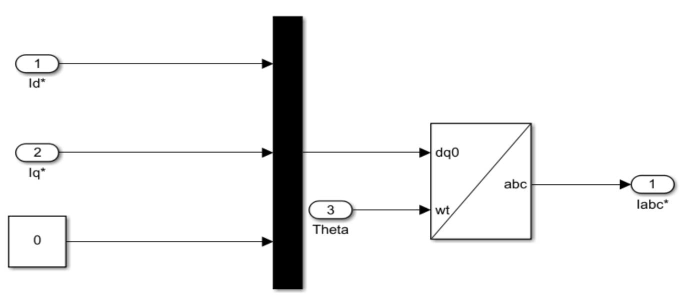

Figure 4.10 Convert current components in rotating frame to three-phase currents in stationary frame

4.2.3.5 Current Regulator

The current regulator shown in figure 4.11 is a feedback current control method where the motor current tracks the reference current within hysteresis band. In this method the reference current is compared to actual motor current. As a result, six pulses are generated to control the switches of inverter in order to provide the motor with desired magnitude and frequency current signals.

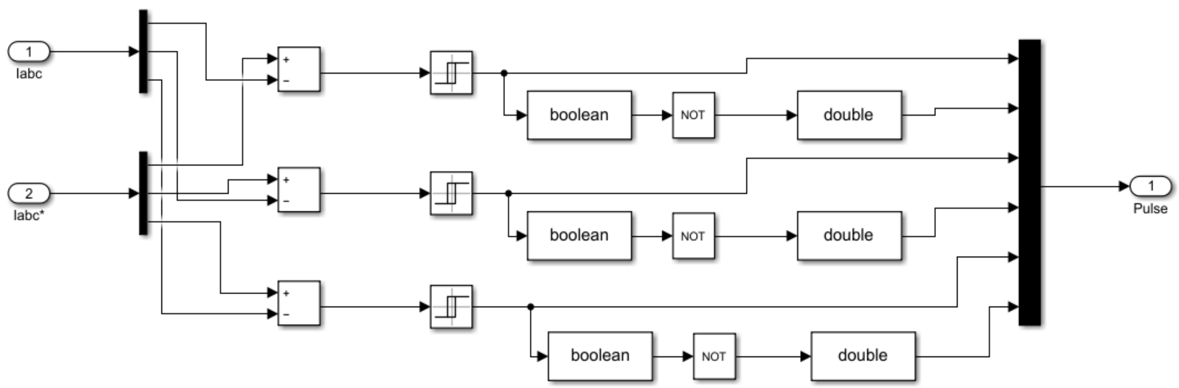

Figure 4.11 SIMULINK model of current regulator

4.2.4 LQR controller Model

The linear quadratic regulator was designed in chapter four of this study. It is based on cost function optimization to obtain optimal control force. To generate the optimal gain matrix *Kopt*, a MATLAB code is used. The MATLAB code is used to generate the optimal gain matrix *Kopt* given the state space equation and the weighting matrices *Q* and R.

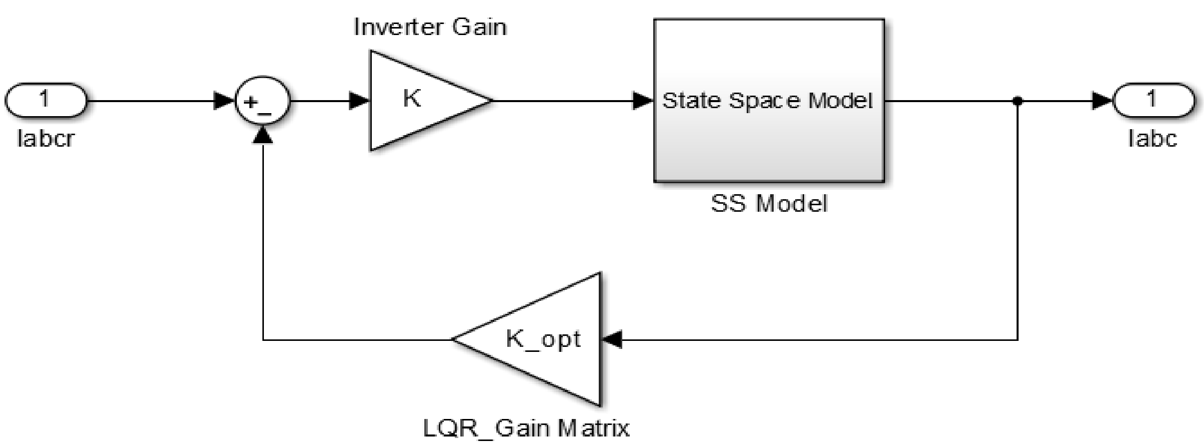

Figure 4.12 Shows how the optimal gain matrix Kopt modeled on Simulink

4.2.5 FLC controller model

The speed error (E) and change in speed error (CE) are input variables in the FLC model, and the reference Torque (T_e*) is an output variable. In a Induction motor drive, the FLC output DU is a change in reference current. To create the actual control signal U (or reference current), the signal is integrated.

The controller analyzes the speed error signal's pattern and updates the output accordingly, ensuring that the actual speed N_act matches the desired speed N_ref.

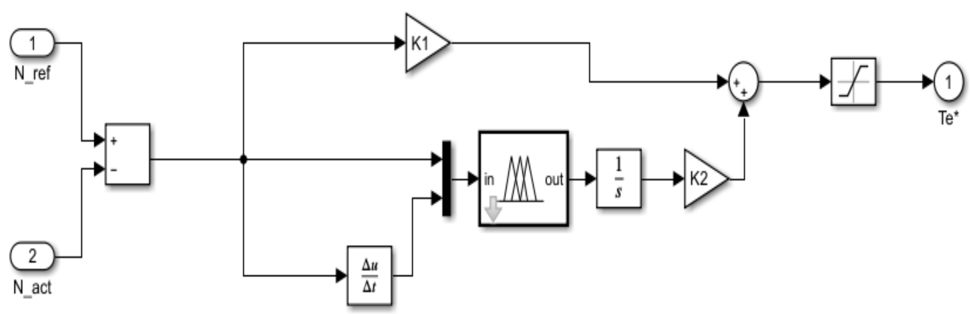

Figure 4.13 FLC for the Induction motor drive system's outer speed loop

4.3. Results and discussions

Under this topic, the simulation results of LQR based Induction motor speed control, fuzzy logic based Induction motor speed control, and Fuzzy-LQR based Induction motor speed control are provided. The two controllers are utilized to track step input individually as well as in combined form in these simulations. Furthermore, under each controller, load torque is applied to the motor abruptly as an external disturbance to test the controller's disturbance handling ability. The performance of each controller is examined based on the performance criteria in order to demonstrate the usefulness of the suggested Fuzzy-LQR control method. Time domain performance evaluations such as percent overshot, rising time, settling time and insensitivity to bounded disturbance, and control input usage (consumption) are the performance measures in this work. Simulations were used to determine the performance evaluation.

4.3.1 Result of LQR based Induction motor controller

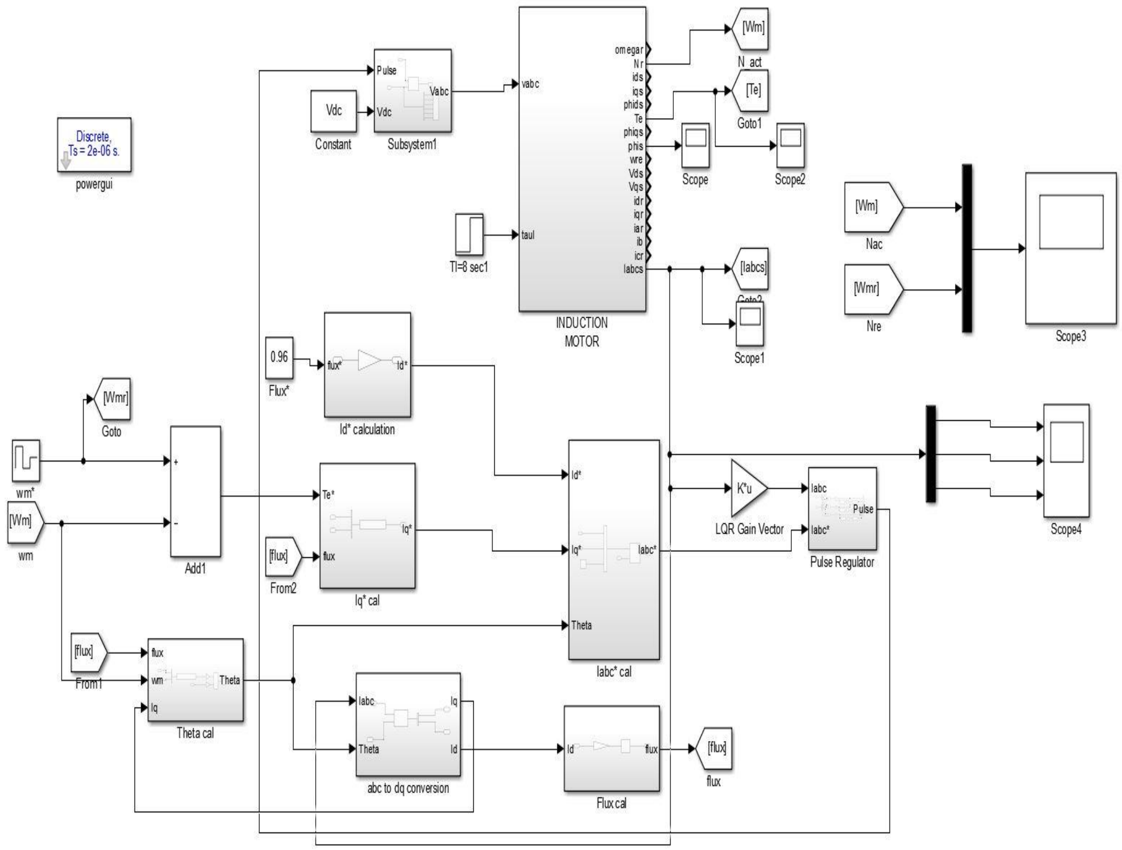

Figure 4.14 Simulink diagram for LQR based Induction motor control

In this simulation, the LQR controller is applied to the inner loop current control and the error amplifier (proportional) gain is applied for the outer speed loop of the drive system. The cost function optimization approach was used to find the optimal gain matrix for the LQR controller. On the other hand, a basic error amplifier (proportional) gain can be achieved by trial and error. The details of the design procedure were presented in chapter three of this thesis. A reference speed stepped to three different values is applied to the drive system. The speed tracking ability of the controller is evaluated against the reference speed based on the time domain performance measures such as settling time, rise time and overshoot. Also, a load torque of 8 Nm is applied as a disturbance input abruptly to the system at a time "t" equal to 1 second. This is to evaluate the disturbance handling ability of the controller. The simulation result of the LQR-based speed control of the Induction motor is shown from Figure 4.15 through Figure 4.18.

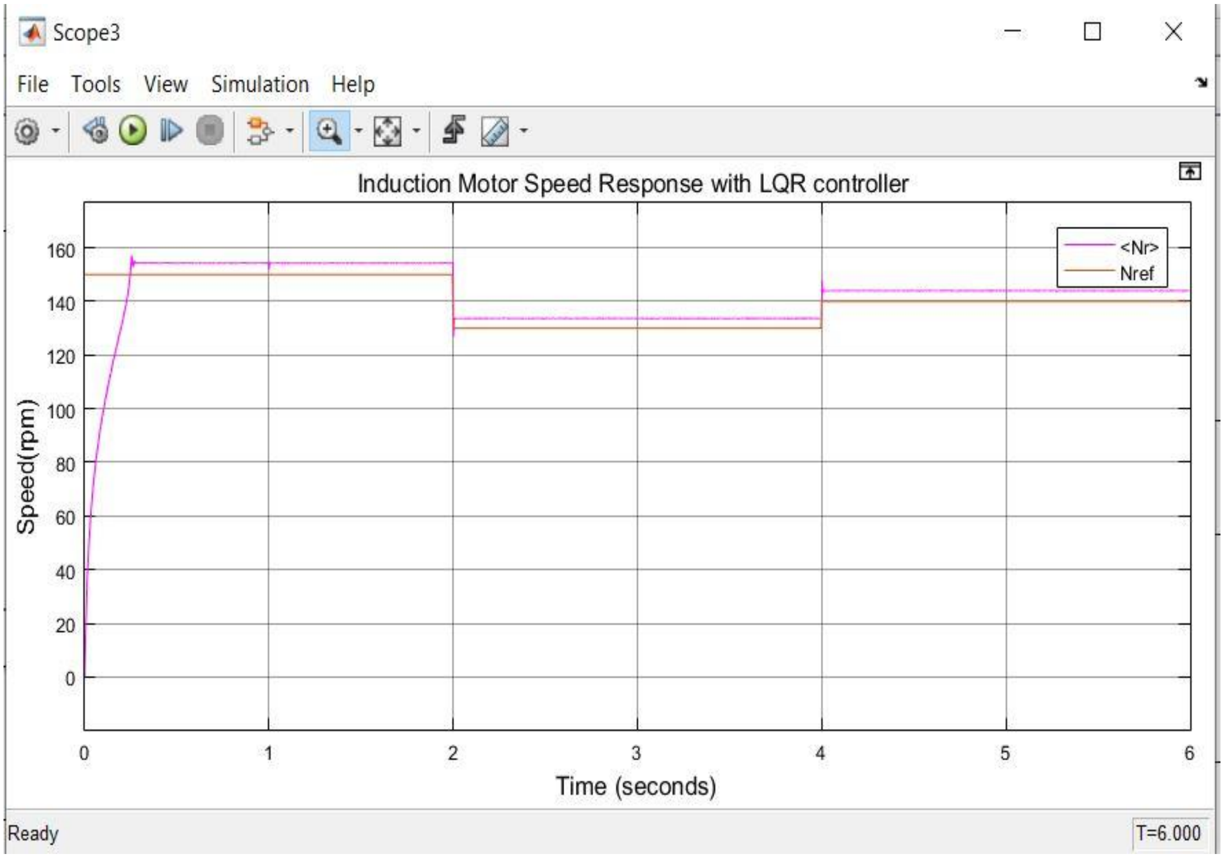

Figure 4.15 Reference speed and actual speed for LQR controlled Induction motor

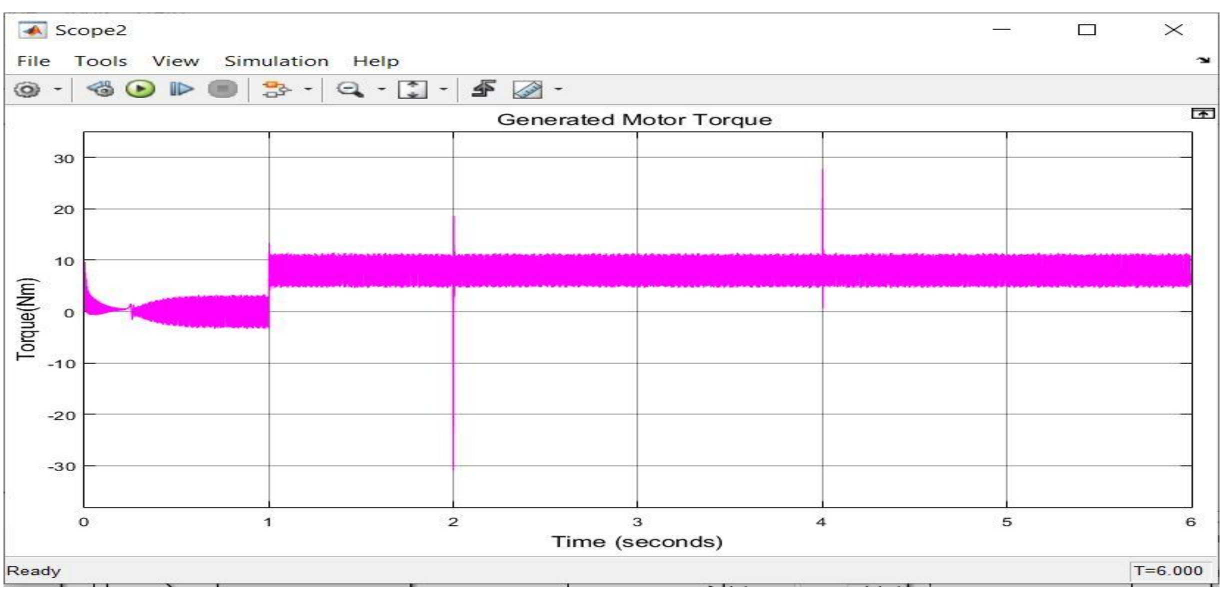

Figure 4.16 Electromagnetic Torque for LQR controlled Induction motor

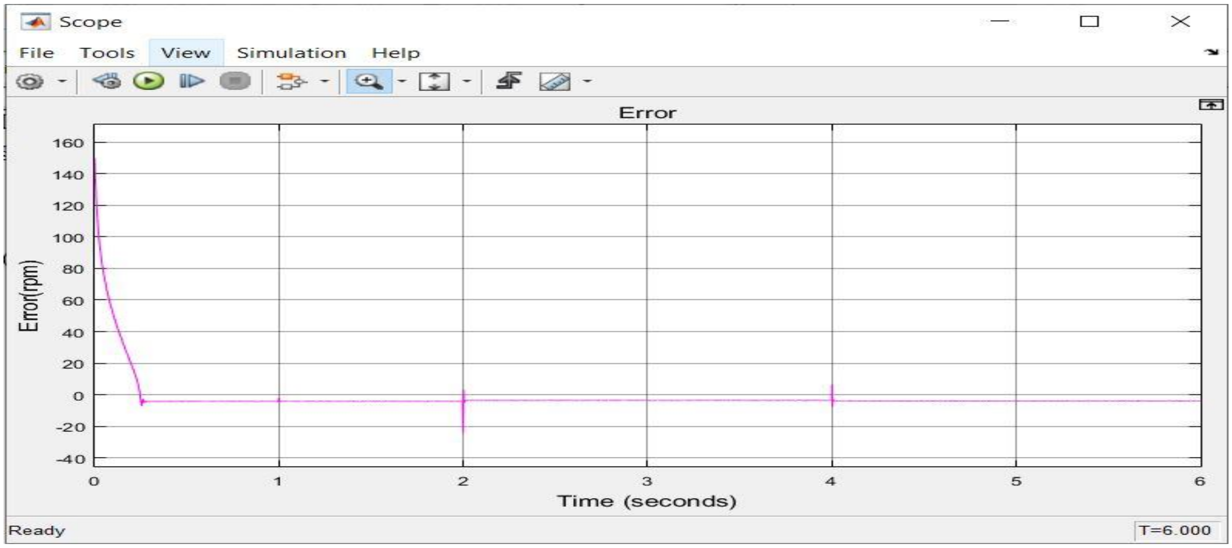

Figure 4.17 Speed Tracking Error

From the simulation results, the speed regulation performance of the LQR controller as shown on Figure 4.15 is satisfactory. The speed response has a 0.151 sec rise time and 20.23% overshot. The result after a load torque of 8 Nm is suddenly applied as a disturbance input at 1 second is also shown on the same figure. From the figure, it is clear that the LQR controller best handles the bounded disturbance load and tracks the reference speed well. The problem with this LQR controller is that the controller uses larger control input for slight deviations from the desired value and causes charting about the desired value. As a result, the cumulative effect of tracking errors will be higher. Figure 4.17 shows how the tracking error behaves due to the chattering effect.

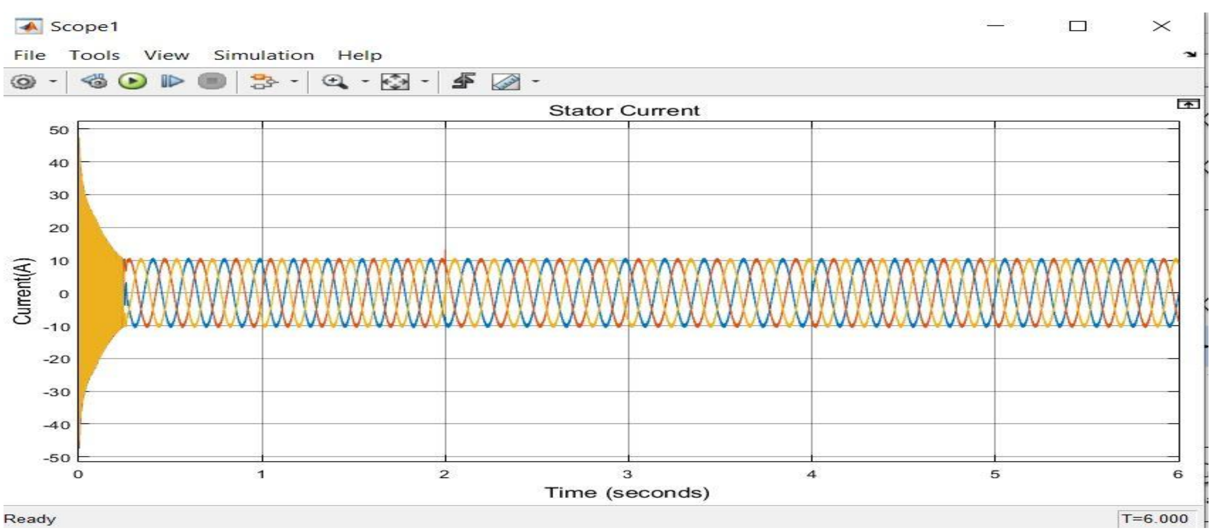

Figure 4.18 Phase stator currents

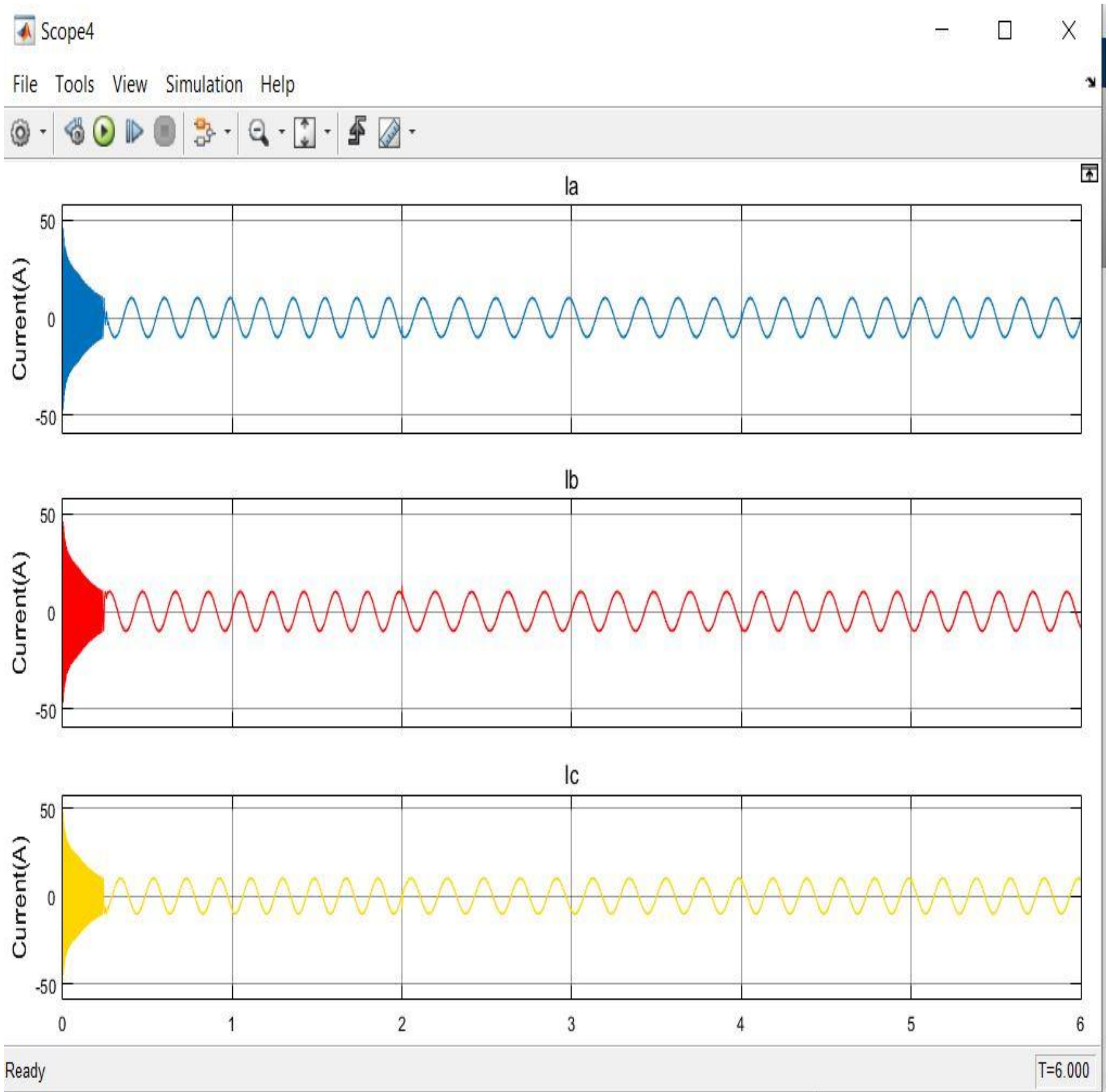

Figure 4.19 Per-phase stator currents

The per-phase stator currents and phase stator currents are shown on Figure 4.18 and Figure 4.19. As seen from the figures, the motor draws large current during starting time and the current is reduced to no load current after the starting period. After the load disturbance is applied, the current is increased to drive the added load.

The torque generated by the motor in response to the applied load torque is depicted in figure 4.16 and is chattered with a higher frequency about the applied load torque. The chattering is due to the aggressiveness of the LQR controller and is undesired.

4.3.2 Result of Fuzzy-logic based Induction motor speed control

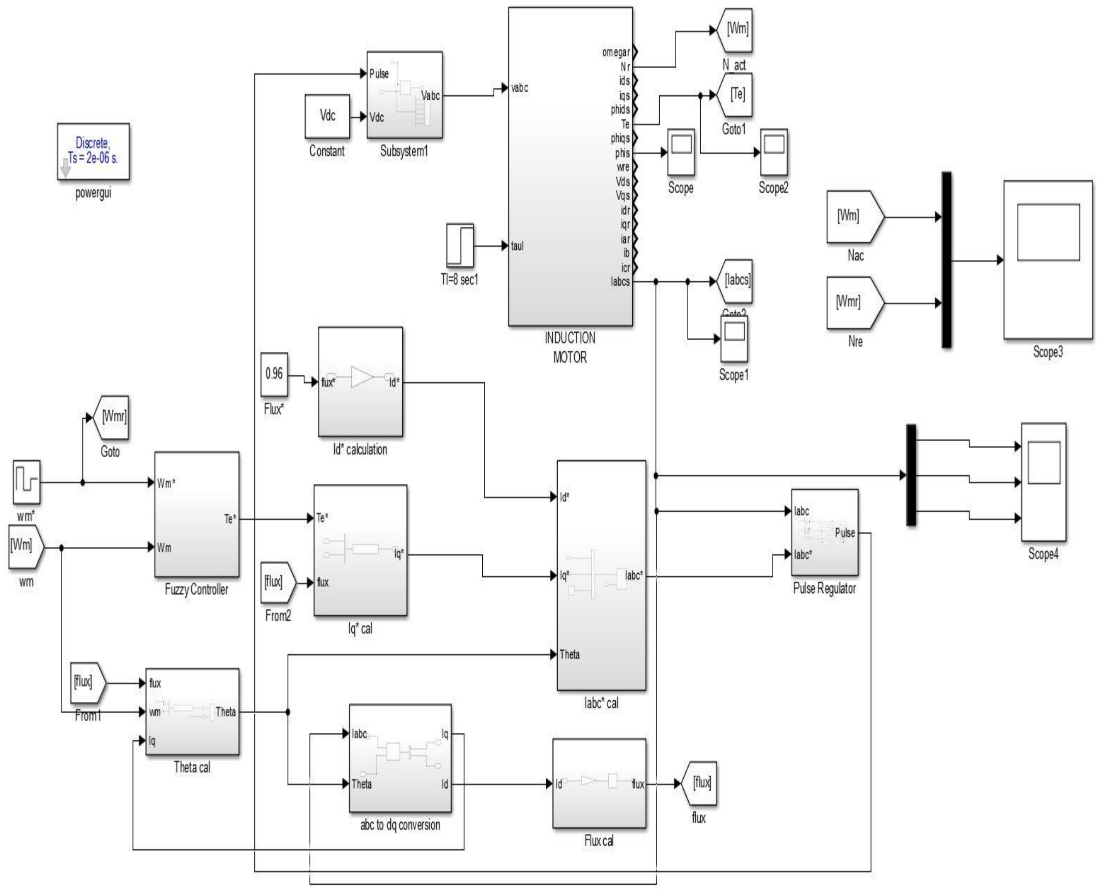

Figure 4.20 Simulink diagram for FLC based Induction motor control

In this simulation, the FLC was applied to the Induction motor drive system. It was applied to the outer speed loop of the drive system to regulate the speed so that a proper control signal was generated and drove the switching of the inverter. The unit feedback system is used in place of the optimal gain matrix here to study the performance of the FLC controller alone. The FLC controller is required to drive and keep the actual speed of the motor at the desired (reference) speed. The drive system is given a reference speed that is stepped through three distinct values. The controller's ability to track a reference speed is evaluated using time domain performance measures such as settling time, rise time, and maximum peak overshot. In addition, at time "t" equal to 1 second, a load torque of 8 Nm is introduced as a disturbance input to the system. This is to evaluate the disturbance handling ability of the controller.

Figures 4.21 through 4.27 show the results for the entire simulation of fuzzy-based speed control.

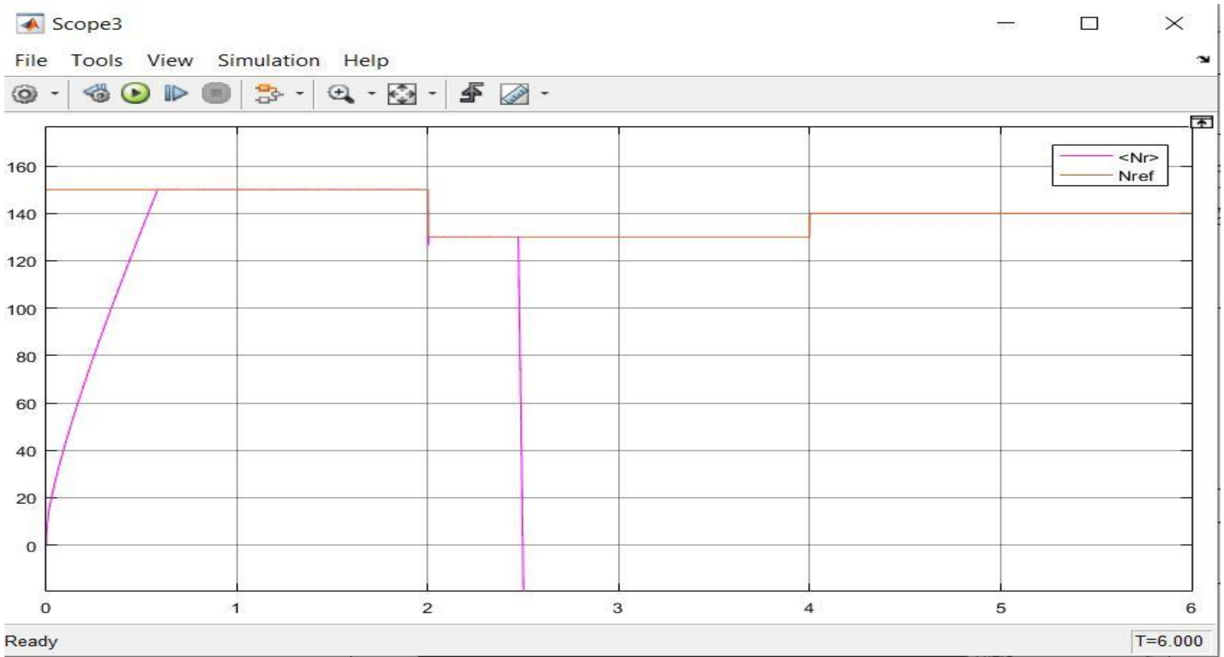

Figure 4.21 Reference speed and actual speed for Fuzzy controlled Induction motor

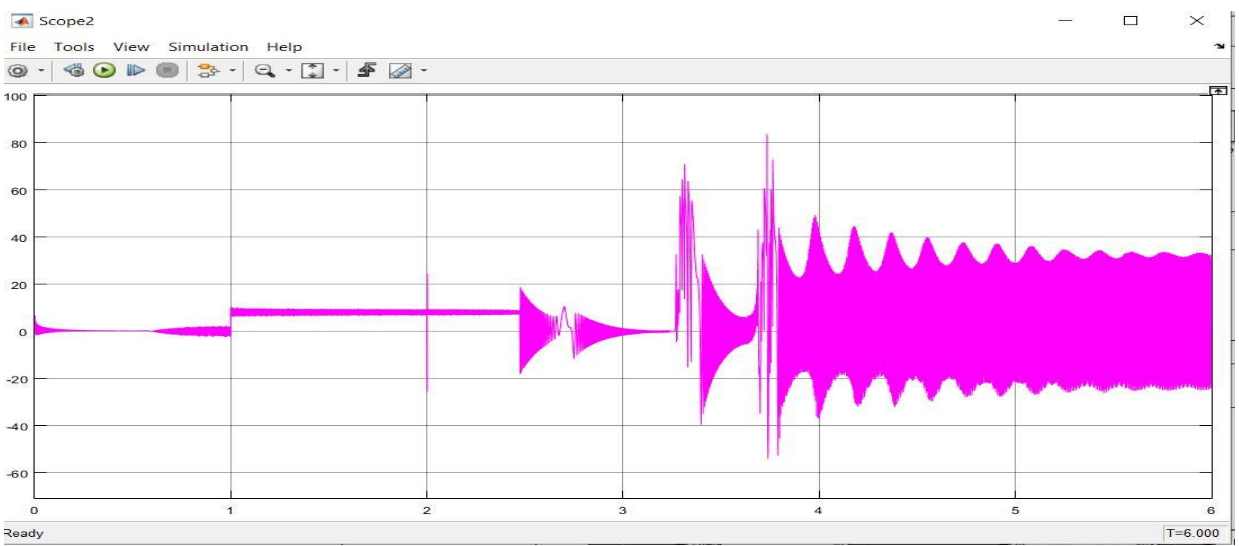

Figure 4.22 Electro Magnetic Torque for Fuzzy controlled Induction motor

The speed response of the FLC controller based Induction motor control is shown on Figure 4.21. The speed response has 0.264 seconds rise time, 0.0149 seconds settling time and an overshoot of 13.83%. The result after a load torque of 8 Nm is suddenly applied as a disturbance input at 1 second is also shown on the same figure. As a result, the actual speed response was reduced. This indicates that the actual speed is lagging behind the reference speed and the controller is not able to reduce the tracking error below the indicated value (see Figure 4.23).

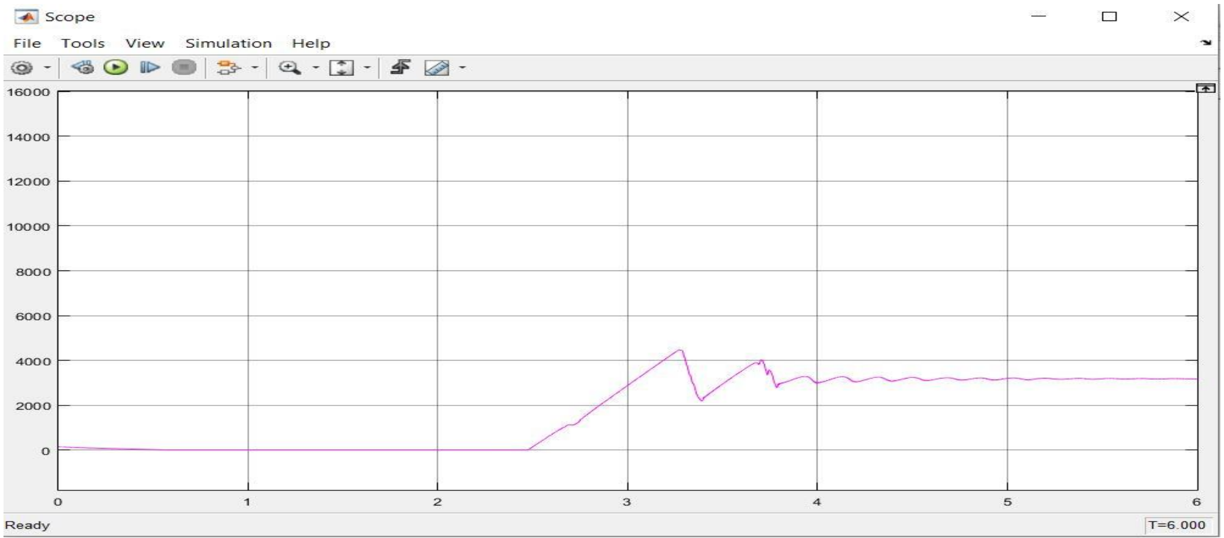

Figure 4.23 Speed Tracking Error

The starting torque, as seen from Figure 4.22, is large and required to turn the rotor from its stationary position. Since no load is applied until 1 second, the electromagnetic torque generated by the motor is no-load torque. After 1 second, since 8 Nm of load torque is applied, the generated electromagnetic torque is increased by the same proportion as the applied load torque.

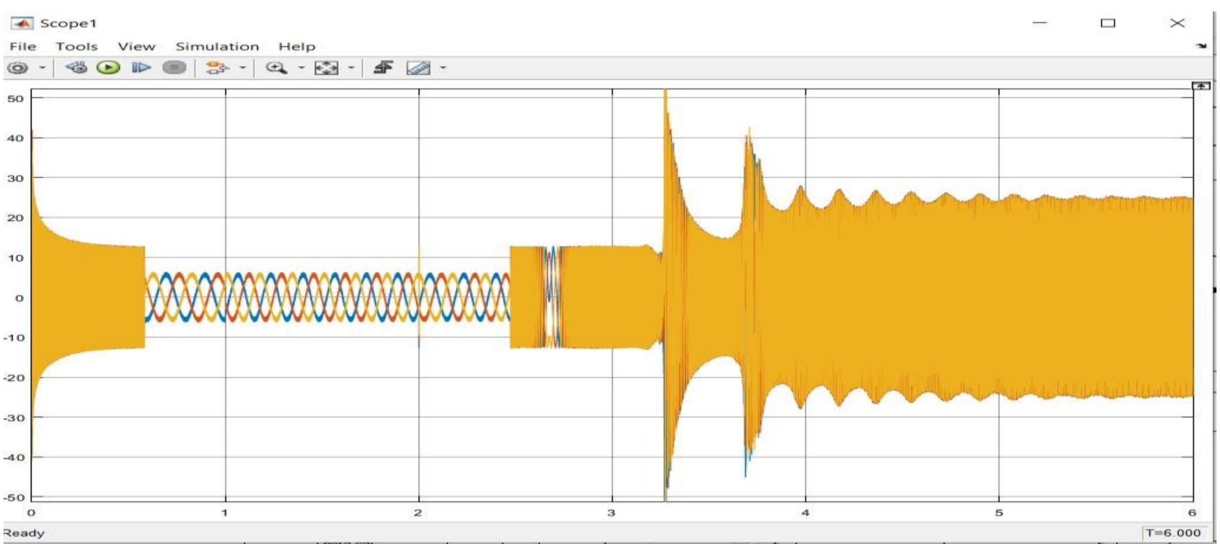

Figure 4.24 Stator phase currents for Fuzzy controlled Induction motor

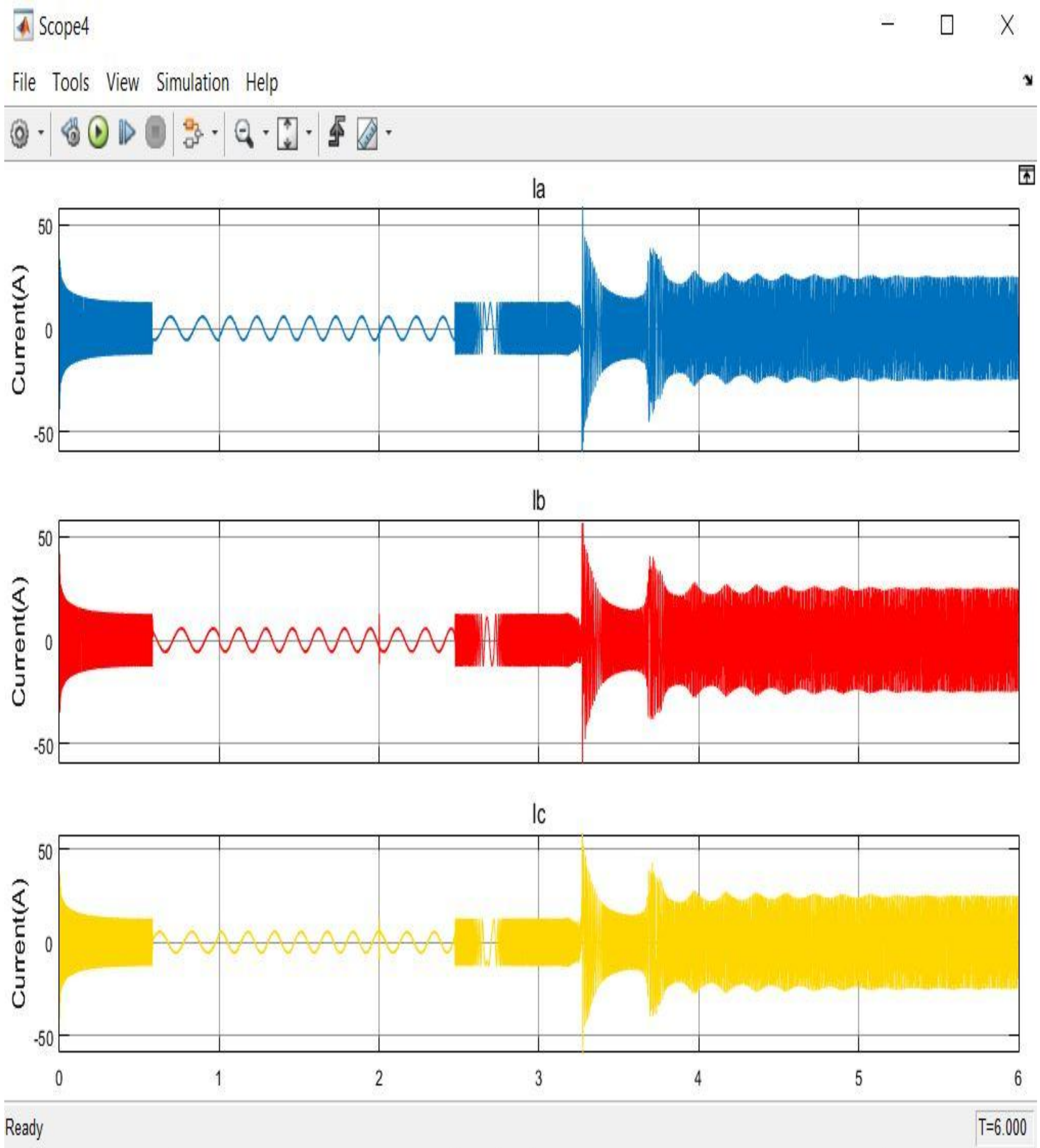

Figure 4.25 Per-phase Stator currents for Fuzzy controlled Induction motor

The three phase stator currents are shown on Figure 4.24 and the per-phase stator currents are shown on Figure 4.25. As seen from the figures, the motor draws large current during starting time and the current is reduced to no load current after the starting period. After the load disturbance is applied, the current is increased to drive the added load.

4.3.3. Result of Fuzzy-LQR based Induction motor speed control

Figure 4.26 Shows Simulink diagram for Fuzzy-LQR based Induction motor speed control.

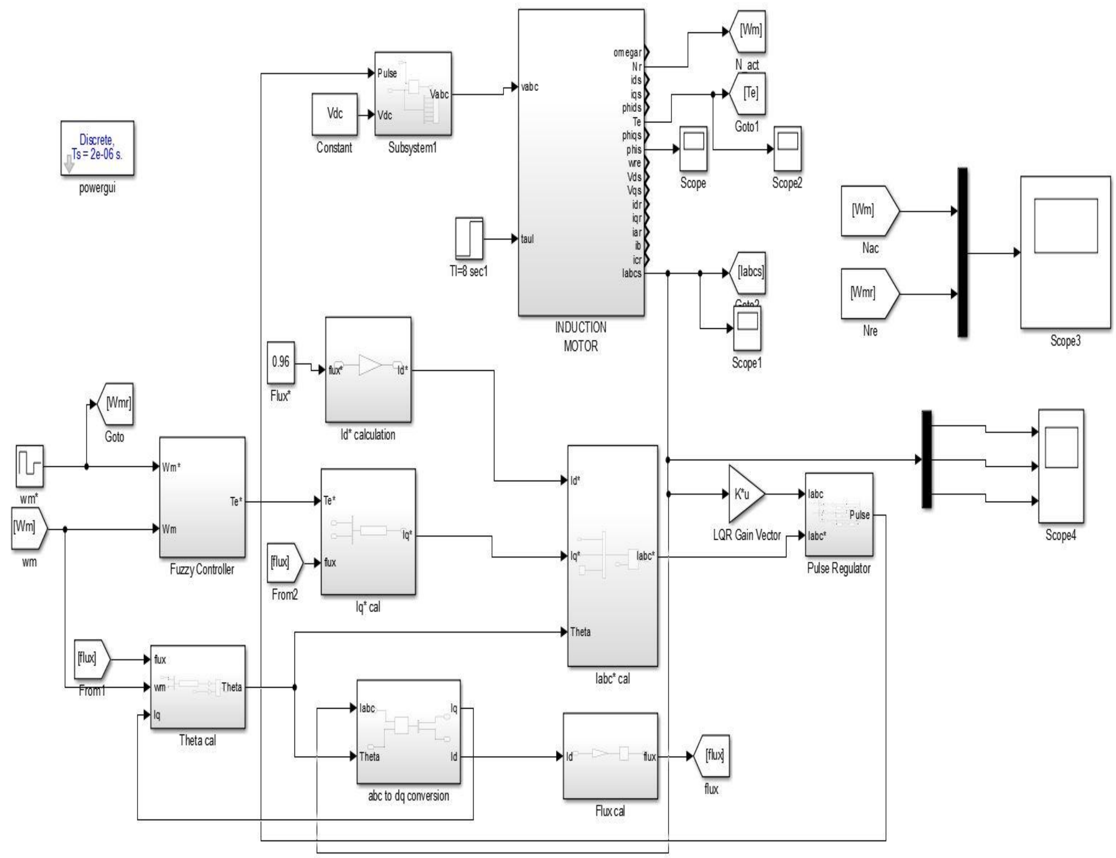

Figure 4.26 Simulink diagram for Fuzzy-LQR based Induction motor control

In this simulation, the FLC is applied to the outer speed loop of the drive system to regulate the speed error so that a proper control signal is generated and drives the switching of the inverter. The LQR controller, on the other hand, is applied to the inner current control loop and the system. The FLC controller is required to drive and keep the actual speed of the motor at the desired (reference) speed. The LQR is also required to maintain the optimal control input force to the Induction motor. Both controllers act simultaneously and hence achieves better performance.

The drive system is required to track a reference speed that is stepped between three distinct values. Based on time domain performance metrics such as settling time, rising time, and overshoot, the controller's speed tracking ability is assessed against the reference speed. In addition, at time "t" equal to 1 second, a load torque of 8 Nm is applied to the system as a disturbance input. The purpose of this test is to see how well the controller handles disturbances. From Figure 4.27 through Figure 4.31, you can see the entire simulation outcome.

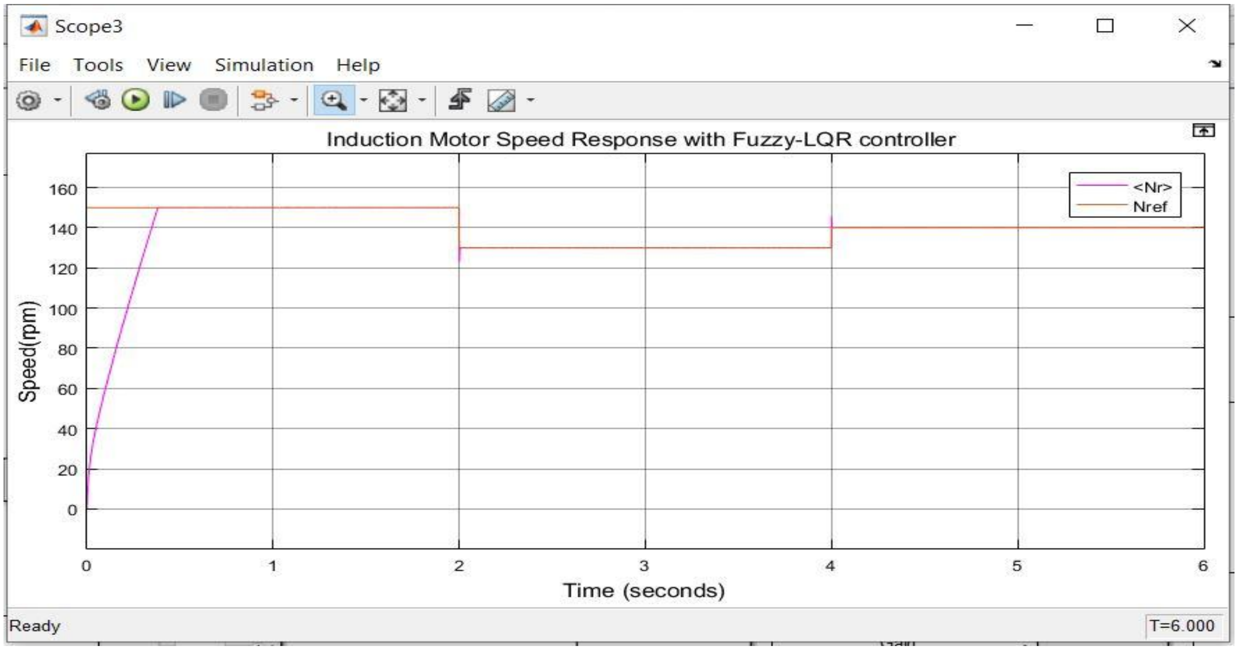

Figure 4.27 Reference speed and actual speed for Fuzzy-LQR controlled Induction motor

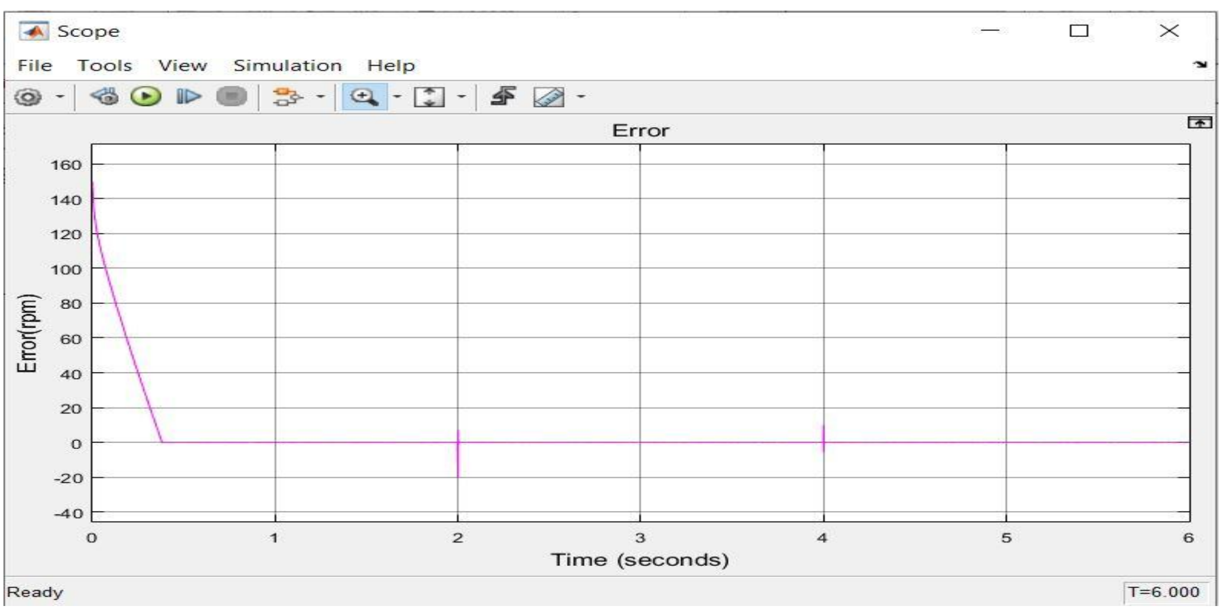

Figure 4.28 Speed Tracking error

Figure 4.27 depicts the speed response of the Fuzzy-LQR control of the Induction motor. The speed response has a rising time of 0.167 seconds, a settling time of 0.0057 seconds, and a maximum peak overshot of 14.77% percent. The speed response after a load torque of 8 Nm is suddenly applied as a disturbance input at 1 second is also undisturbed and properly tracks the desired speed input. This effect is shown in Figure 4.30, which is the speed tracking error, and has a value of approximately 0.1 RPM, which is almost negligible as compared to the actual speed.

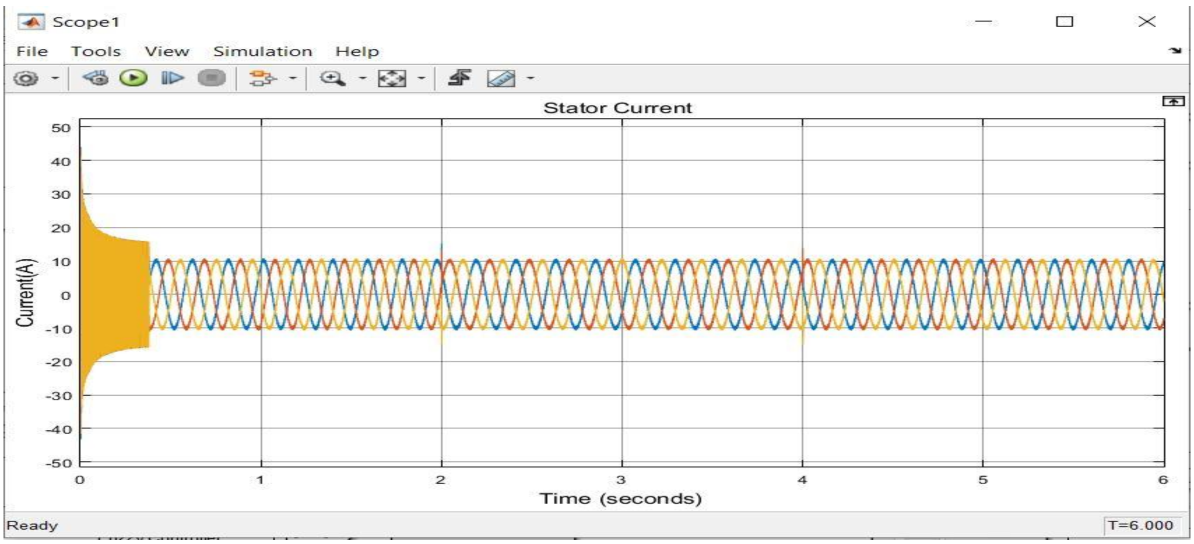

Figure 4.29 Three phase stator current

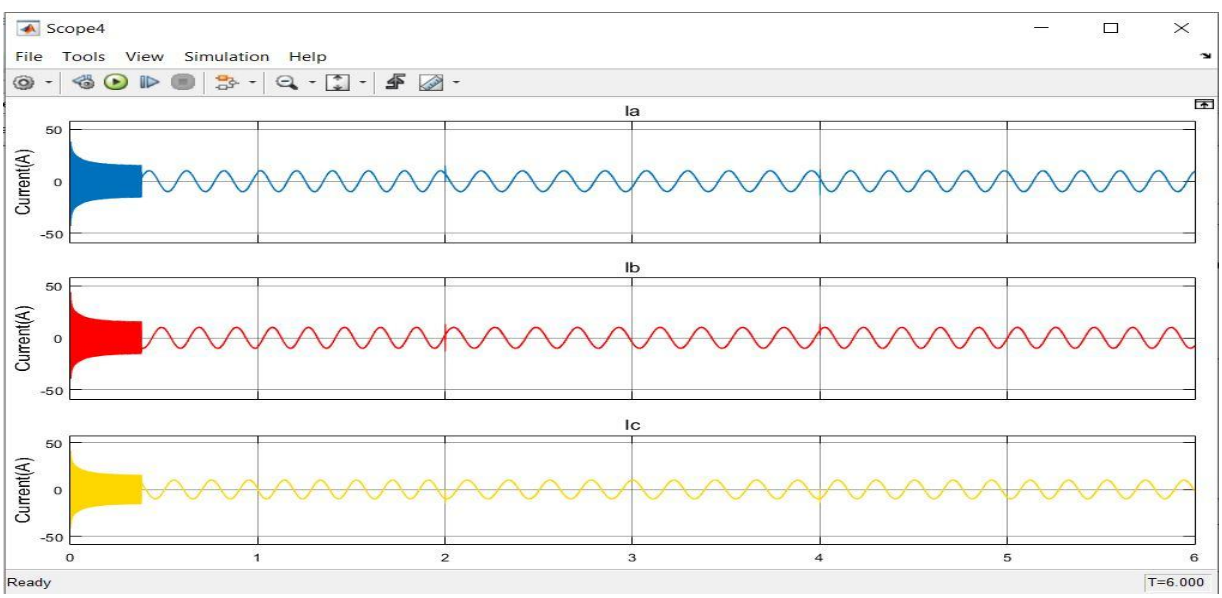

Figure 4.30 Per-Phase Stator Currents *Ia*,*Ib* and *Ic*

Figure 4.31 Applied load torque at 1 second and electromagnetic torque produced similarly, the starting torque (see Figure 4.31) is large and required to turn the rotor from its stationary position. Since no load is applied until 1 second, the electromagnetic torque generated by the motor is no-load torque. A load torque of 8 Nm is applied, and the generated electromagnetic torque is increased. Moreover, the electromagnetic torque generated is free from chattering.

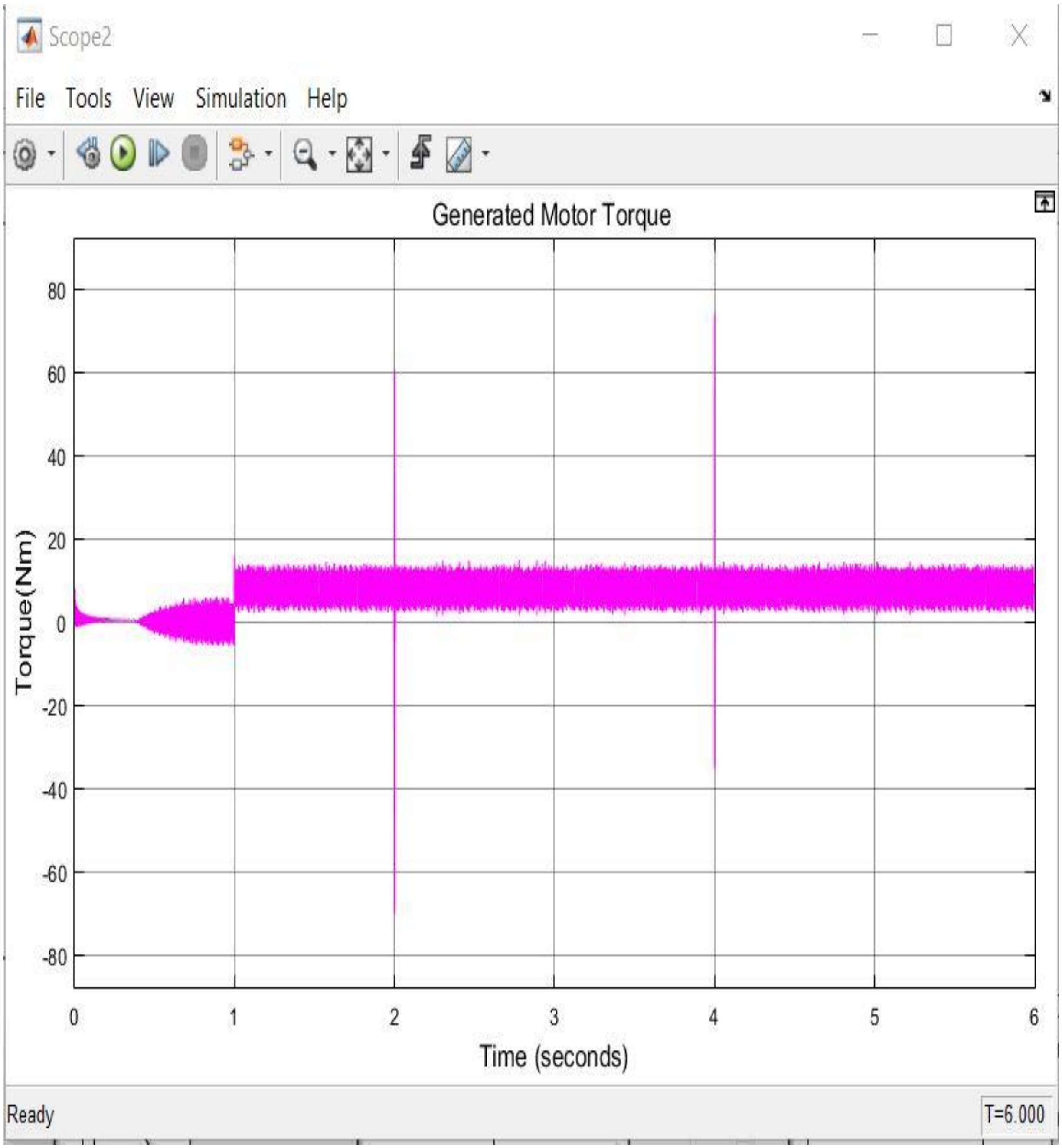

Figure 4.31 Electromagnetic Torque of Fuzzy-Lqr controller

Table 4.2 summarizes the results obtain in the simulation and is the base for evaluating the performance of the controllers.

Table 4.2 List of performance attained by each controller

Performance measures	LQR	FLC	Fuzzy-LQR
Rise time in (seconds)	0.151	0.264	0.167
Settling time in (seconds)	0.0182	0.149	0.0057
Overshoot in (%)	20.23	13.83	14.77
Tracking error before disturbance torque applied	Good	Excellent	Excellent
Tracking error after disturbance torque applied	Excellent	Moderate	Excellent
Disturbance handling capacity	Excellent	Moderate	Excellent
Control force utility	Higher	Optimal	Optimal

Based on the summary of the results in Table 4.2 and the tracking error comparison, the FLC controller has good response time with minimum overshot but is unable to completely eliminate the effect of disturbance load. LQR, on the other hand, is the fastest and also eliminates the effect of disturbance load. But it uses large control force for slight deviations from the desired response and hence creates chattering. Fuzzy-LQR reduced the overshoot, eliminated the chattering effect and resulted in a smooth speed response with the least tracking error, utilizing optimal control force, and hence was selected as the best of the mentioned controllers.

CONCLUSIONS AND RECOMMENDATIONS

Conclusion

In this thesis work, a Fuzzy-LQR based speed control technique for Induction motor drive systems has been presented and has been simulated successfully. The study attempts to improve the performance of the Induction motor by ensuring optimal control input utility and smooth speed trajectory tracking even in the presence of disturbance. Both FLC and LQR based speed control techniques were individually simulated to evaluate the proposed Fuzzy-LQR controller. Simulation was carried out using MATLAB/SIMULINK. In each case, a reference speed that is stepped through three distinct values has been applied to be tracked by the response of the respective controller. Also, a load torque of 8 Nm is applied as a disturbance input abruptly to the system at time "t" equal to 1 second to evaluate the disturbance handling abilities of the controllers. Finally, evaluation against the reference speed has been done for each case based on the time domain performance measures such as settling time, rise time and overshoot. The result for the suggested Fuzzy-LQR control shows a speed response rise time of 0.167 seconds, a settling time of 0.0057 seconds, and an overshoot of 14.77 percent. The speed response is also undisturbed after an 8 Nm load torque is applied as a disturbance input at 1 sec, and it tracks the desired speed input properly. Furthermore, the current drawn by the stator phases is smooth and stepped, just as the Induction motor requires for smooth operation. Thus, by means of the simulation example, it has been shown that the goal of enhancing the performance of the Induction motor is achieved by applying the proposed Fuzzy-LQR controller that ensures the utilization of optimal control force (input) that enables the motor to smoothly track the desired speed command and also makes it more resilient to load disturbances.

Recommendation

As observed based on the simulation of the study, it is better to implement a Fuzzy-LQR controller for the Induction motor drive system to improve the performance of the motor by ensuring optimal control input utilization that will drive the system smoothly even in the presence of disturbance. In this study, the design of optimal LQR is done by selecting the weighting matrices R and Q through trial and error, but it is recommended that it's better to use other weight selection techniques like algebraic LQR weight selection algorithms. Also, to make the controller more advanced, it's better to include an artificial neural network (ANN) so that it can learn and update the weights of each rule to bring out the best output from the fuzzy inference system.

References

Agrawal, L. K. (2018). Speed control of brushless DC motor using Fuzzy controller. *International Journal of Pure and Applied Mathematics*, 119(15), 2689-2696.

Aktaibi, A. &. (2011). Dynamic simulation of a three-phase induction motor using matlab simulink. . *currents*,, 8, 9.

Aktas, M. A. (2020). Direct torque control versus indirect field-oriented control of induction motors for electric vehicle applications. *Engineering Science and Technology,an International Journal*, 23(5), 1134-1143.

Babu, P. N. (2019). An adaptive differentiation frequency based advanced reference current generator in grid-tied PV applications. *IEEE Journal of Emerging and Selected Topics in Power Electronics*, 8(4), 3502-3515.

Bernal, E. L. (2021). Optimization of type-2 fuzzy logic controller design using the GSO and FA algorithms. *International Journal of Fuzzy Systems*, 23, 42-57.

Dias, F. J. (2022). *Performance comparison of superconducting machines with induction motors.* IEEE Transactions on Applied Superconductivity.

Farah, N. T. ((2019)). A novel self-tuning fuzzy logic controller based induction motor drive system: An experimental approach. *IEEE Access*, 7, 68172-68184.

Hussien, M. G. (2019, December). Mathematical Analysis of the Small Signal Model for Voltage-Source Inverter in SPMSM Drive Systems. *In 2019 21st International Middle East Power Systems Conference (MEPCON)* (pp. pp. 540-549). IEEE.

Jung, J. H. (2019, August)). uzzification: Anti-Fuzzing Techniques. In USENIX Security Symposium. pp. 1913-1930).

Karaboga, D. &. (2019). Adaptive network based fuzzy inference system (ANFIS) training approaches: a comprehensive survey. *Artificial Intelligence Review*, 52, 2263-2293.

Kotsur, M. Y. (2018, February). Speed synchronization methods of the energy-efficient electric drive system for induction motors. *In 2018 14th International Conference on Advanced*

Trends in Radioelecrtronics, Telecommunications and Computer Engineering (TCSET) (pp. pp. 304-307). IEEE.

Kumar, S. &. (2020, June). Different Control Scheme for the Quadcopter: A Brief Tour. *In 2020 First IEEE International Conference on Measurement, Instrumentation, Control and Automation (ICMICA)* (pp. pp. 1-6). IEEE.

Lam, C. S. (2020). Hysteresis current control of hybrid active power filters. *IET Power Electronics*, 5(7),1175-1187.

Leedy, A. W. (2022, April). Simulink/MATLAB dynamic induction motor model for use in undergraduate electric machines and power electronics courses. (pp. 1-6).

Lipo, T. A. (2017). *Introduction to AC machine design.* John Wiley & Sons.

Maharajan, M. P. (2018). Design of speed control and reduction of torque ripple factor in BLDC motor using spider based controller. IEEE Transactions on Power Electronics.

Metha, V. R. (2018, October). Speed control of induction motor using a fuzzy logic controller and direct torque controller. *In 2018 4th International Conference for Convergence in Technology (I2CT)* (pp. pp. 1-5). IEEE.

Neupane, S. (2023, 04 12). *OnlineStudent Guide*. Retrieved from onlinestudentguide.com: https://onlinestudentguide.com/three-phase-induction-motor-construction/

Nik Badrul Alam, N. M. (2021). Time series forecasting model based on intuitionistic fuzzy set via equal distribution of hesitancy de-i-fuzzification. I, Fuzziness and Knowledge-Based Systems,. *nternational Journal of Uncertainty*, 29(06).

Okyere, E. B. (2019). LQR controller design for quad-rotor helicopters. *The Journal of Engineering*, 4003-4007.

Okyere, E. B. (2019). LQR controller design for quad-rotor helicopters. *The Journal of Engineering*, 2019(17), 4003-4007.

Rajpoot, S. C. (2018). *Speed Control of Three Phase Motor Using Fuzzy Logic Controller.*

Rajput, S. B. (2020). Simplified algorithm for assessment equivalent circuit parameters of induction motors. *IET Electric power applications*, , 14(3), 426-432.

Samavat, T. N. (2023). A Comparative Analysis of the Mamdani and Sugeno Fuzzy Inference Systems for MPPT of an Islanded PV System. *International Journal of Energy Research*, 20.

Song, X. C. (2020). Research on performance of real-time simulation based on inverter-dominated power grid. 9, .1137-1153.

Swargiary, M. D. (2017, September). Sensorless stator field-oriented digital control of induction motor based on LQR theory with augmented integral error. *In 2017 IEEE International Conference on Power, Control, Signals and Instrumentation Engineering (ICPCSI)*. IEEE.

Wang, K. L. (2018). An improved indirect field-oriented control scheme for linear induction motor traction drives. *IEEE Transactions on Industrial Electronics*, 65(12), 9928-9937.

Yassine, B. F.-A. (2019, March). New MRAS Approach for Sensorless control of IM. *In 2019 19th International Conference on Sciences and Techniques of Automatic Control and Computer Engineering (STA)* (pp. pp. 36-40). IEEE.

Zand, M. N. (2021, February). Robust speed control for induction motor drives using STSM control. *In 2021 12th Power Electronics, Drive Systems, and Technologies Conference (PEDSTC)* (pp. pp. 1-6). IEEE.

Zaparoli, I. O. (2020). Transient envelope current analysis for inter-turn short-circuit detection in induction motor stator. *Journal of the Brazilian Society of Mechanical Sciences and Engineering*, 42(2), 1-12.

APPENDIX

Appendix A

A.1: Induction Parameter setting on MATLAB:

```
% Parameters of a typical induction machine.
rs=1.405; %Stator resistance
rr=1.395; %Rotor resistance
Ls=0.178039; %Stator inductance
Lr=0.178039; %Rotor inductance
M=0.1722; % Mutual inductance
K1= 75.46; % By trial and error
K2= 3.25;
K_opt= diag([ 2.543 2.543 2.543]);
P=4;    %Poles
J=0.0131; %Inertia
sigma=(Ls*Lr)-(M*M);
B=0.1;
sls=sigma/Lr;
tr=Lr/rr;
sigma1=sigma/(Lr*Ls);
c1=(Lr/M);
c2=(Ls*Lr-M*M)/(M);
lst=sigma/Lr;
```